

Electronic Supplementary Information

**Continuous flow processing of bismuth-photocatalyzed atom
transfer radical addition reactions using an oscillatory flow
reactor**

Pauline Bianchi,^a Jason Williams^{*a,b} and C. Oliver Kappe^{*a,b}

^a*Institute of Chemistry, University of Graz, NAWI Graz, Heinrichstrasse 28, 8010 Graz, Austria*

^b*Center for Continuous Flow Synthesis and Processing (CCFLOW), Research Center Pharmaceutical Engineering GmbH (RCPE),
Inffeldgasse 13, 8010 Graz, Austria*

*E-mail: jason.williams@rcpe.at; oliver.kappe@uni-graz.at

Contents

Contents	2
A. General experimental information	3
A.1. Materials and methods	3
A.2. Batch setup	5
A.3. Oscillatory flow photoreactor setup	6
B. Reaction optimization	8
B.1. Batch optimization.....	8
B.1.1. Preliminary batch trials.....	8
B.1.2. Physicochemical properties of Bi_2O_3	9
B.1.3. Laser diffraction experiments.....	9
B.1.4. GC analysis of the model reaction.....	10
B.1.5. Control reaction for homogeneous catalysis	12
B.2. Flow optimization.....	13
B.2.1. Design of the flow setup.....	13
B.2.2. Residence time distribution	15
C. Process Mass Intensity (PMI) calculation.....	17
D. Scope – Procedures and characterization data	18
E. NMR spectra	22
F. References	30

A. General experimental information

A.1. Materials and methods

Bismuth(III) oxide (Sigma Aldrich, powder of 10 μm particle size, 99.9% trace metals basis and nanopowder of 90-210 nm particle size, 99.8% trace metals basis, CAS 1304-76-3), 2,6-lutidine (Sigma Aldrich, 98%, CAS 108-48-5), decane (Sigma Aldrich, 98%, CAS 124-18-5), 1-hexene **1a** (TCI, >97%, CAS 592-41-6), diethyl bromomalonate **2a** (TCI, >85%, CAS 685-87-0), allylbenzene **1b** (TCI, >98%, CAS 300-57-2), allyl alcohol **1c** (Fluka, 98%, CAS 107-18-6), 1-hexyne **1d** (TCI, >97%, CAS 693-02-7), bromoacetonitrile **2b** (TCI, >97%, CAS 590-17-0), perfluorohexyl iodide **2c** (Acros, 97%, CAS 355-43-1), carbon tetrabromide **2d** (Sigma Aldrich, 99%, CAS 558-13-4), polyethyleneglycol 400 (Sigma Aldrich, CAS 25322-68-3) and acetone (technical grade) were received from commercial sources and used without further purification.

Samples were analyzed by **gas chromatography (GC)** in a Shimadzu GC FID 230 gas chromatograph with a flame ionization detector (FID). Helium, used as the carrier gas (40 cm sec⁻¹ linear velocity), goes through a RTX-5MS column (30 m \times 0.25 mm ID \times 0.25 μm). The injector temperature is set to 280 °C. After 1 min at 50 °C, the temperature is increased by 25 °C min⁻¹ to 300 °C, then held for 4 min at 300 °C. The gases used in the detector for flame ionization are hydrogen and synthetic air (5.0 quality).

Particles were centrifuged in an Eppendorf Centrifuge 5804. Solutions were concentrated under reduced pressure in a Heidolph rotatory evaporator. Thin-layer chromatography (TLC) analyses were performed on Merck pre-coated TLC plates (silica gel 60 GF254, 0.25 mm) with UV light (254 nm) or KMnO₄ stain solutions as visualizing/developing agents. Chromatographic purification was performed on a Biotage Isolera automated flash chromatography system using cartridges packed with 25 g of KP-SIL, 60 Å (32–63 μm particle size). The eluent was a mixture of 40–60 petroleum ether and ethyl acetate (95:5 or 50:50).

NMR analysis was carried out on a Bruker 300 MHz spectrometer (¹H: 300 MHz, ¹³C: 75 MHz). The chemical shifts of ¹H and ¹³C are given in ppm relative to residual signals of the solvent (CDCl₃ at 7.26 ppm for ¹H NMR and 77.2 ppm for ¹³C NMR). Coupling constants are given in Hertz (Hz). Multiplicity is indicated with the following abbreviations: s, singlet; d, doublet; t, triplet; q, quartet; m, multiplet.

Laser diffraction (LD) analysis was carried out on a Sympatec Helos H2395 particle sizing instrument. For size measurements, approximately 5 mg of solid was added to 50 mL of acetone in a cuvette. The sample in the cuvette was stirred at 1500 rpm during measurements. Two separate 30 s

measurements were taken, to cover a combined particle size range of 0.45-875 μm . For suspendability measurements, approximately 5 mg of the solid was added to 50 mL of the desired solvent mixture in a cuvette (optical density $\sim 28\%$), stirring at 1500 rpm. Upon starting measurements, stirring was stopped and the measurement of optical density was recorded every second for 20 s. This procedure was performed 5 times for each sample, providing average values at each time point.

High-resolution mass spectrometry (HRMS) measurements were carried out with an Agilent 6230 TOF mass spectrometer, after separation of the compounds with an Agilent 1260 Infinity Series HPLC-system. The injection volume is set to 0.5 μL and the flow rate to 0.3 mL min^{-1} of a mixture of 40% H_2O (0.1% 5 M Amminoumformiate) and 60% $\text{ACN}/\text{H}_2\text{O}$ (5:1 +0.1% 5 M Amminoumformiate). The HRMS module comprises an electrospray ionization source (Dual AJS ESI) and uses nitrogen as the nebulizer (15 psig) and the drying gas (5 L min^{-1}). ESI experiments were performed using the positive ionization mode (Gas Temp. = 300 $^\circ\text{C}$, Fragmentor = 150 V, Skimmer = 65 V, OCT 1 RF V_{pp} = 750 V, V_{cap} = 1400, Nozzle Voltage = 2000 V, Reference Masses = 121.050873 and 922.009798, Acquisition = 100-1,100 m/z , 1 spectra s^{-1}).

A.2. Batch setup

A sealed vial purged with argon was placed at the bottom of a magnetic stirrer (Fig S1). An LED module equipped with 50 W LEDs of 400 or 455 nm and a cooling system (Fig S2 for the emission spectra of each LED) was placed at 10 cm from the vial.

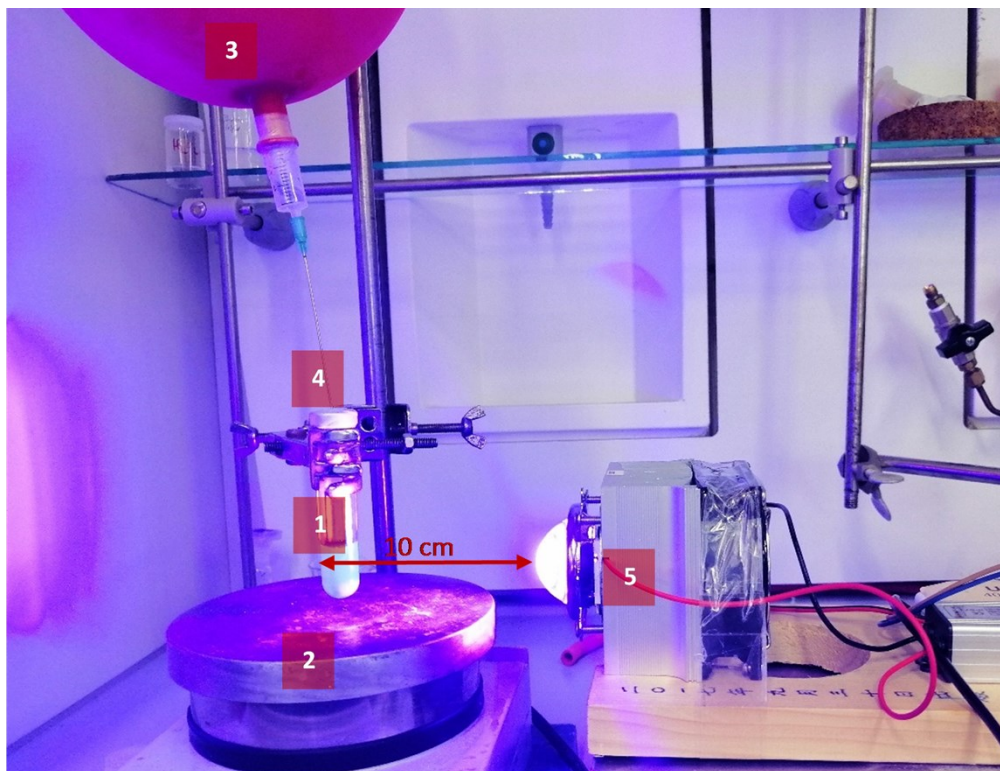


Fig. S1 Batch setup for the ATRA reaction. **1** vial with a magnet and the reaction mixture; **2** magnetic stirrer; **3** Ar balloon; **4** septum + needle; **5** 50 W LED with a cooling system.

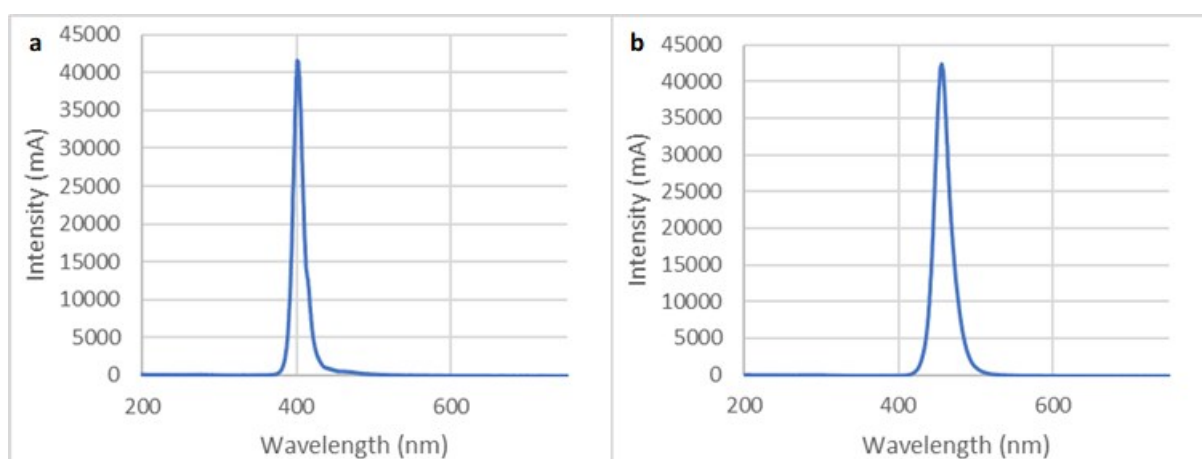


Fig. S2 Emission spectra of the 50 W LEDs used during batch optimization. **(a)** 400 nm. **(b)** 455 nm.

A.3. Oscillatory flow photoreactor setup

A flow setup consisting of two pumps, an oscillatory flow reactor, an LED module, thermostats, vibrating motors, and a back pressure regulator was designed to enable the efficient handling of Bi_2O_3 particles even at a low flow rate (Fig. S3).



Fig. S3 General continuous flow setup for the ATRA reaction photocatalyzed by Bi_2O_3 particles. **1** magnetic stirrer; **2** reaction mixture; **3** metering peristaltic pump (SF-10, Vapourtec); **4** pulsator (Creaflow customized ProMinent (beta/4) pump with PTFE/carbon pump head); **5** HANU reactor; **6** Peschl LED module (405 nm); **7** BPR (Swagelok, 5 bar); **8** collection vessel; **9** Huber cryostat; **10** LED cooling system; **11** Vibrators

Reactor module: All flow experiments were performed in a commercially available plug flow HANU reactor (HANU HX 15-C276-CUB reactor, Creaflow) which consists in a Hastelloy baseplate composed of a series of cubic static mixing elements within a flow channel (530 mm × 60 mm × 45 mm size; 2 mm × 2mm × 2 mm static mixing elements; 480 mm × 17 mm glass window; 2 mm × 2 mm channel dimensions; 15 mL internal volume).

Light source: An LED module (“novaLIGHT FLED75” water-cooled high-performance LED array, Peschl Ultraviolet) equipped with 36 LEDs of 405 nm (maximum current = 700 mA; radiation flow at maximum current = 45 W; width at 50% intensity = 15 nm, Fig. S4) and placed at the top of the reactor for visible light irradiation.

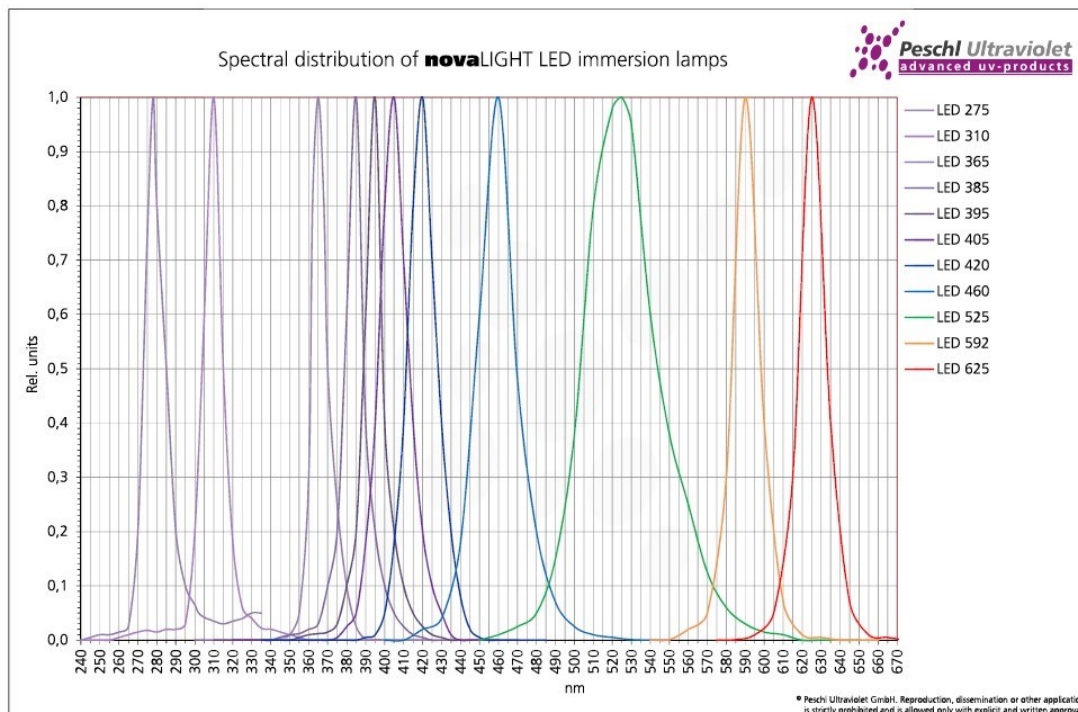


Fig. S4 Emission spectra of LEDs used (405 nm for this process). **Note:** intensities are normalized.

Peristaltic pump: The feed mixture was pumped through a Vapourtec SF-10 peristaltic pump (0.02-10.00 mL min⁻¹; blue peristaltic tubing).

Oscillatory pump: The oscillations were provided by a pulsator (ProMinent Beta/4 pump, PTFE/carbon pump head, customized by Creaflo), which was placed between the reactor and the peristaltic pump. The tunable frequencies can vary from 0.3 to 3 Hz (10 to 100%) while the amplitudes can be tuned from 0.04 to 0.44 mL (<5 to 100%) per stroke.

Back pressure regulator: A pressure of 5 bar was maintained using a Swagelok back pressure regulator (KCB Series, Stainless Steel Compact BP Regulator, 0 to 375 psig (25.8 bar), 1/8 in. FNPT), placed at the end of the setup.

Thermal regulation: Thermal regulation of the reaction path was achieved with a Huber CC304 thermostat filled with silicon oil (temperature range -20 °C to 195 °C).

Connections: All connections between the parts of the setup are made using 1/8" (1.6 mm i.d.) and 1/16" (0.8 mm i.d.) o.d. PTFE/PFA tubes with PEEK or stainless steel (Swagelok) fittings.

B. Reaction optimization

B.1. Batch optimization

B.1.1. Preliminary batch trials

Table S1 Preliminary trials of the batch ATRA reaction between **1a** and **2a**

Entry	Solvent	[1a] (M)	[2a] (M)	Bi ₂ O ₃ size (mol%)	Additive (equiv.)	λ_{irr} (nm)	t (h)	T (°C)	Color	Conv. (%)	Yield (%)
1 ^b	acetone	0.594	0.44	210 nm (1)	/	455	20	rt	yellow/orange (turbid)	<1	<1
2 ^b	acetone	0.594	0.44	10 μ m (1)	/	455	20	rt	yellow	93	92
3 ^c	acetone	0.5	0.5	10 μ m (1)	lutidine (1)	455	20	rt	beige (turbid)	90	89
4 ^c	acetone	0.44	0.5	10 μ m (1)	lutidine (1)	455	20	rt	beige (turbid)	67	67
5 ^d	acetone	0.675	0.5	10 μ m (1)	lutidine (1)	455	20	rt	beige (turbid)	>99	98
6 ^d	acetone	0.675	0.5	10 μ m (5)	lutidine (1)	455	20	rt	grey (turbid)	6	6
7 ^e	acetone	1.35	1	10 μ m (1)	lutidine (1)	455	20	rt	beige (turbid)	67	67
8 ^e	acetone	1.35	1	10 μ m (0.5)	lutidine (1)	455	20	rt	beige (turbid)	63	63
9 ^f	acetone	0.675	0.5	10 μ m (1)	lutidine (1)	455	5	rt	beige (turbid)	<1	<1
10 ^f	acetone	0.675	0.5	10 μ m (1)	lutidine (1)	400	5	rt	beige (turbid)	>99	98
11 ^g	acetone	0.675	0.5	/	lutidine (1)	455	20	rt	orange	<1	<1
12 ^g	acetone	0.675	0.5	10 μ m (1)	lutidine (1)	/	20	rt	beige (turbid)	<1	<1

^a consumption of starting material **2a** and yield of desired product **3a**, based on GC-FID area with decane as the internal standard ^b effect of the particle size; ^c effect of the stoichiometry of **1a** vs **2a**; ^d effect of the catalyst loading; ^e effect of the concentration; ^f effect of the wavelength (5h instead of 20 h of irradiation); ^g control tests

B.1.2. Physicochemical properties of Bi_2O_3



Fig. S5 Physicochemical properties of Bi_2O_3 particles. **(a)** reaction with HBr and prevention with the addition of 2,6-lutidine. **(b)** reduction into Bi^0 in various solvents. From left to right: acetone; acetone:PEG 400 (8:2); acetone:ethylene glycol (8:2); benzyl alcohol. **(c)** effect of the particle size on the color of the solution.

B.1.3. Laser diffraction experiments

The size of Bi_2O_3 particles that were used during this protocol (10 μm according to Sigma Aldrich) was determined through laser diffraction experiments (Fig. S6). A volumetric mean diameter was centered at 13.8 μm , with a median particle diameter of 13.4 μm .

$D_{10} = 6.72 \mu\text{m}$; $D_{50} = 13.40 \mu\text{m}$; $D_{90} = 21.44 \mu\text{m}$.

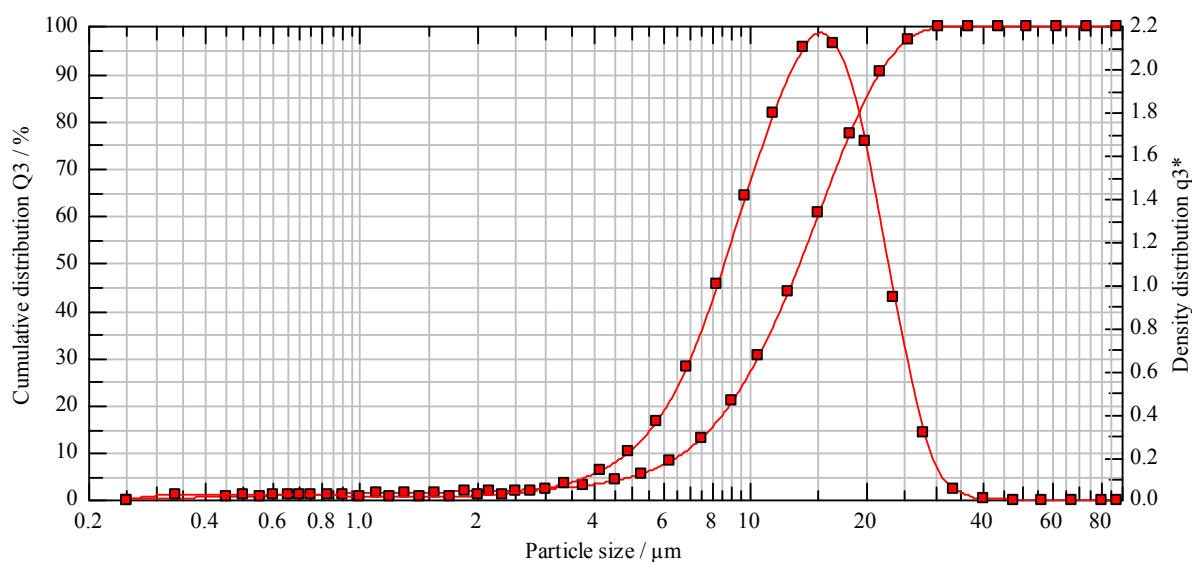


Fig. S6 Particle size profile of 10 μm Bi_2O_3 particles from sigma Aldrich obtained from laser diffraction experiments.

Laser diffraction experiments were also needed to select the loading and chain length of PEG. After stopping to stir a mixture of acetone and PEG containing 5 mg of Bi_2O_3 particles, the optical density was measured over 20 s. The slower the decrease in optical density, the slower the particles were deposited at the bottom of the vessel, hence showing better particle suspendability (Fig. S7).

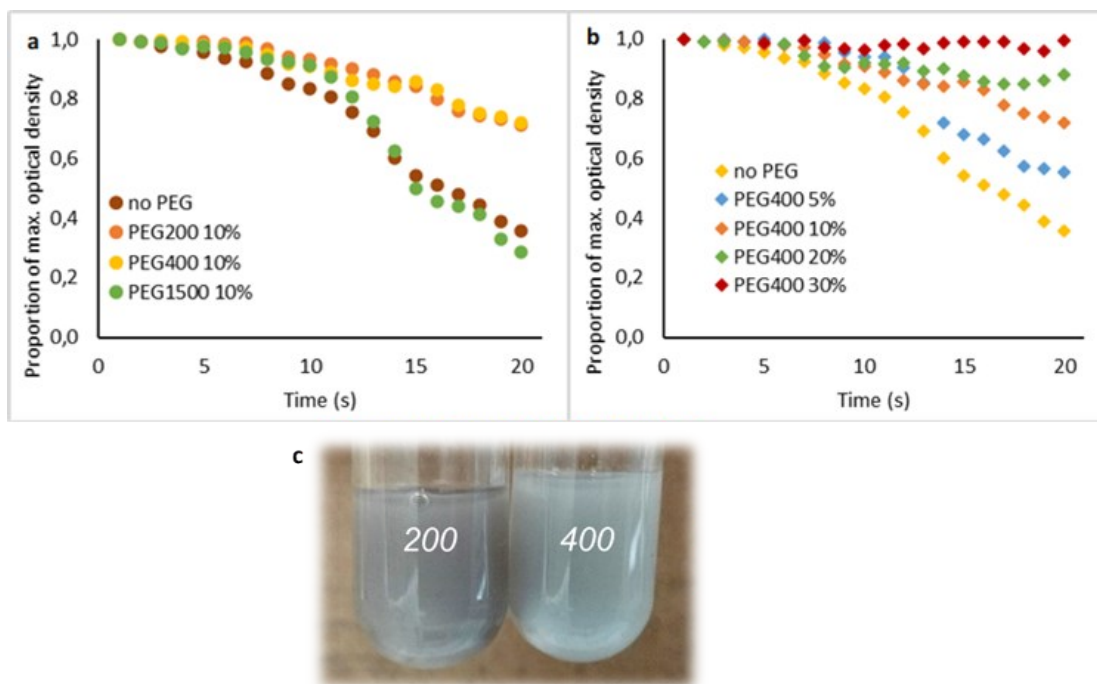


Fig. S7 Optical density over time after stirring of samples containing Bi_2O_3 particles in various mixtures of acetone and PEG. **(a)** effect of the PEG chain length. **(b)** effect of the PEG loading. **(c)** Mixture of acetone:PEG 200 (left) or acetone:PEG 400 (right) containing 5 mg of Bi_2O_3 after 5 h of irradiation at 400 nm

From Fig. S7a, it appeared that short chain lengths improve particle suspendability, while large ones deleted the beneficial effect of adding PEG in the solution. From Fig. S7b, the trend shows that it was better to have a high amount of PEG to avoid particles settling. To decide between PEG 400 and PEG 200, two mixtures of acetone with 20% of PEG 400 or PEG 200 and Bi_2O_3 particles were irradiated at 400 nm. Higher content of Bi^0 was obtained with PEG 200 than with PEG 400, probably due to the higher content of free OH functionalities. Therefore, a mixture of acetone:PEG 400 8:2 in volume was chosen as the ideal solvent for heterogeneous ATRA reactions under continuous flow conditions.

B.1.4. GC analysis of the model reaction

The model reaction between **1a** and **2a** was monitored by GC-FID. The optimization of the reaction conditions led to the disappearance of the signal for **2a** at 6.175 min and the appearance of three peaks: the major one for **3a** at 8.662 min and two minor ones that could be related to elimination products at 7.597 and 7.664 min (Fig. S8). Conversions of **2a** and yields of **3a** were calculated through calibration curves with decane as the internal standard (IS), following equation 1 (Fig. S9). The same monitoring and calibrations curves were used for the flow experiments.

$$[\text{analyte}] = \left(\frac{\text{Area}_{\text{analyte}}}{\text{Area}_{\text{IS}}} - c \right) * \frac{[\text{IS}]}{k} \quad (\text{Equation 1})$$

where k is the slope and c the intersection with the y -axis

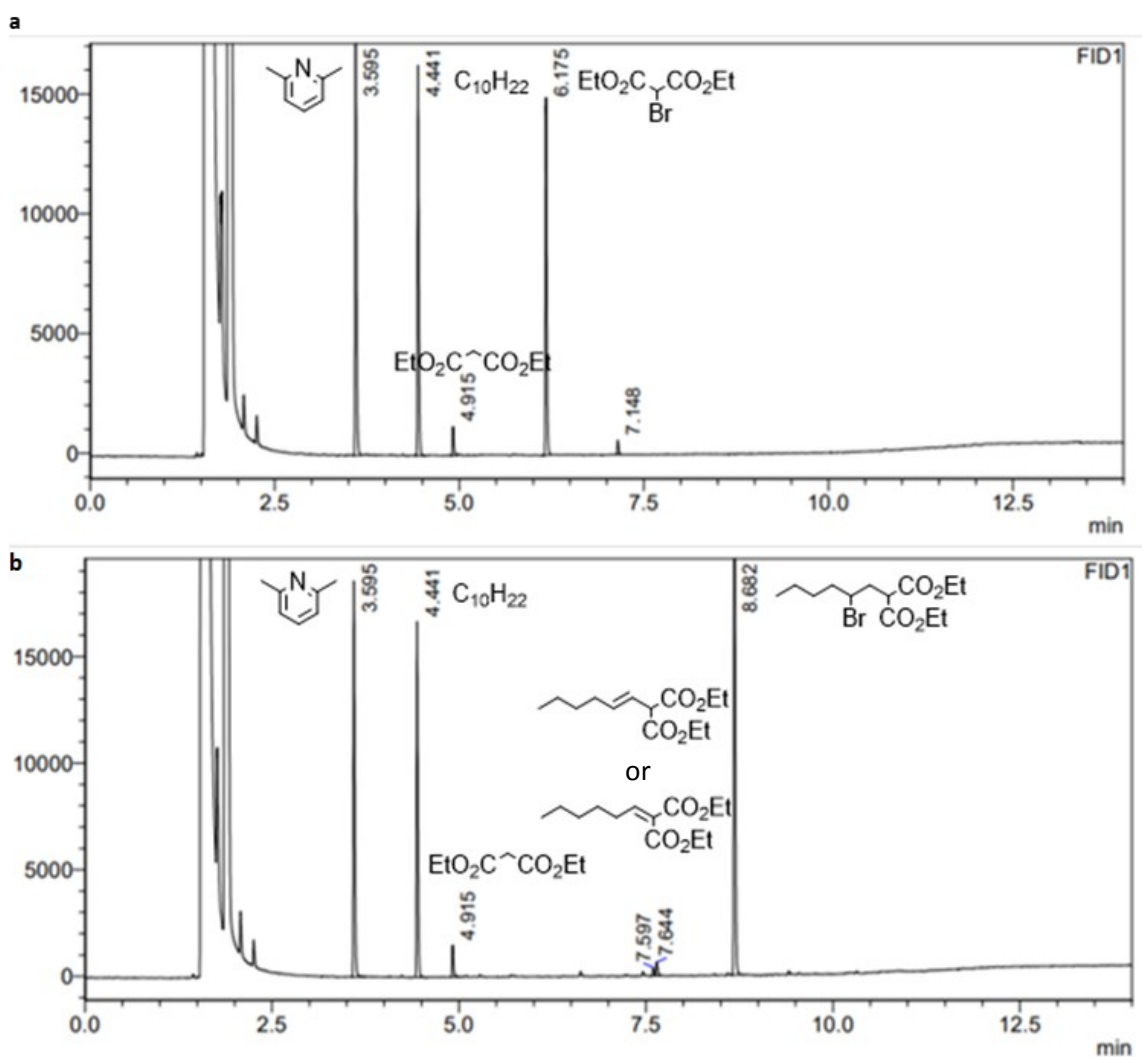


Fig. S8 GC analysis of the model reaction under the optimized batch conditions. **(a)** Spectrum before reaction. **(b)** Spectrum after 5 h of irradiation at 400 nm

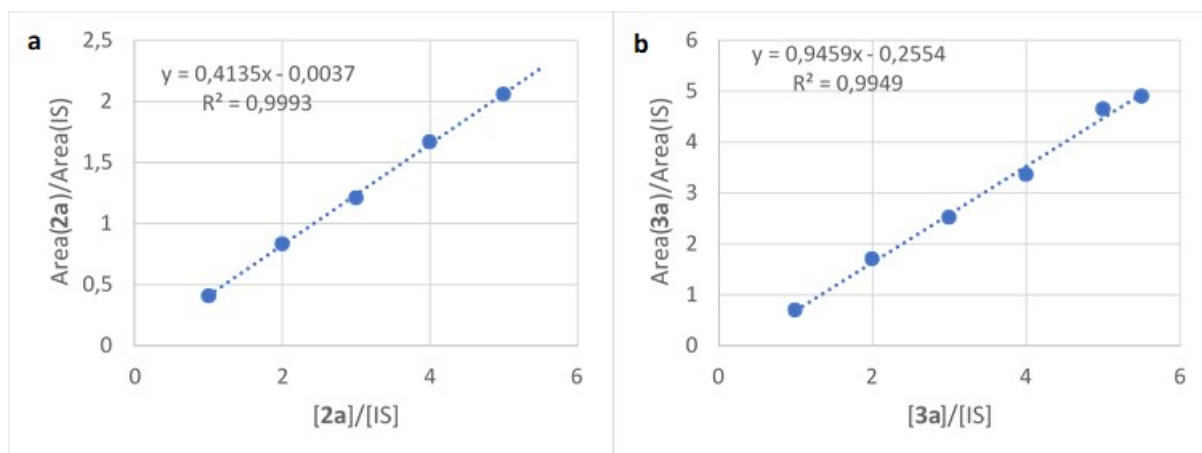


Fig. S9 GC-FID calibration curves vs decane (IS) for the model reaction. **(a) 2a (b) 3a**

B.1.5. Control reaction for homogeneous catalysis

As described in the manuscript, an additional experiment was carried out, to test for homogeneous catalysis. This was set up using the representative batch procedure, detailed in the manuscript. After 2 h, the reaction mixture was sampled for GC analysis, then removed from the microwave vial and filtered through a syringe filter (0.45 μm) to remove heterogeneous Bi_2O_3 . The clear solution was then added to a new (argon-flushed) microwave vial and irradiated for a further 3 h before further GC analysis.

Table S2. Results of control experiment for homogeneous catalysis, demonstrating that further reaction is observed after filtration of solids.

Reaction time (h)	Conversion (%)^a	Yield 3a (%)^a
0	0	0
2 (reaction mixture filtered)	5	4
5	76	71

^a consumption of starting material **2a** and yield of desired product **3a**, based on GC-FID area with decane as the internal standard

The reaction clearly shows further progress after the filtration step, but does not reach complete conversion, as is seen after 5 h under optimal reaction conditions. This implies that there is homogeneous catalysis at work and the observed induction period may be due to the time required for functionalization (or simply dissolution) of Bi_2O_3 particles.

B.2. Flow optimization

B.2.1. Design of the flow setup

The most challenging concept to manage during the transposition to continuous flow conditions was avoiding particles settling, since Bi_2O_3 is a dense solid ($d = 8.9 \text{ g cm}^{-3}$). That is why some aspects had to be considered:

- A. *Increasing the solvent viscosity:* already determined during the batch optimization, it is known that the higher the solvent viscosity (μ), the better the suspension. This can be easily proven through the Stokes number (Stk, Equation 2)⁵¹ that shows the behavior of particles suspended in a fluid flow. The lower this number, the better the particles follow the fluid stream. Therefore, the mixture of acetone:PEG 400 (8:2 in volume) was chosen as the solvent.

$$\text{Stk} = \frac{t_p}{t_F} = \frac{\rho_p d_p^2 u}{18 \mu d_h} \quad (\text{Equation 2})$$

(t_p = particle relaxation time (s), t_F = characteristic flow time (s), u = flow velocity (m s^{-1}), d_h = characteristic dimension (m), d_p = particle diameter (m), ρ_p = particle density (kg m^{-3}), μ = viscosity (Pa s))

- B. *Decreasing the particle size:* in the same idea, decreasing the particle diameter (d_p) decreases the Stokes number so it enhances the particle suspension. In this context, however, the smaller particles were found to be less reactive and were sticking along the polymer tubing connecting the reactor. Therefore, only the large particles (10 μm of diameter) were used for the optimization under flow conditions.
- C. *Increasing the particle loading:* according to Slavnić et al.,⁵² increasing the solid loading (mp) increases the viscosity of the mixture and prevents particles depositing (Equation 3). However, the tendency of Bi_2O_3 to be reduced must still be taken into account during the flow setup design. That is why the catalyst amount was increased from 1 mol% to 2 mol%.

$$\mu_m = \mu_l 10^{\frac{1.82 mp}{\rho_p V_R}} \quad (\text{Equation 3})$$

(μ_m = viscosity of the mixture (Pa s)), (μ_l = viscosity of the liquid (Pa s)),
 ρ_p = particle density (kg m^{-3}), mp = mass of the particles collected, V_R = volume of the reactor)

- D. *Designing the most suitable oscillatory flow setup*

D.1. Flow photoreactor: a specially designed commercial oscillatory flow reactor was used, see section A.3 for details.

D.2. Pumps: two pumps were used during this project. The first one was a peristaltic pump (Fig. S10a), responsible for the net flow. Since this one is made of a rotor with rollers, which compress a flexible tube where the solution passes through, this kind of pump enables the handling of solids, which is not the case with many other types of pumps. The second one was an oscillatory pump (Fig. S10b) enabling the application of oscillations with tunable frequencies and amplitudes. The inlet and outlet tubes for this pump had to be oriented vertically to avoid settling inside.

D.3. Tube diameter: it is better to decrease the tube diameter (**D**), since it enables a better solid suspension. According to the Reynolds number, which indicates the ratio of inertial to viscous forces in a net flow, using thinner tubes decreases the Reynolds number so it lowers the impact of the inertial forces in the Stokes regime (see Equation 4).

$$Re_n = \frac{u\rho D}{\mu} \quad (\text{Equation 4})$$

(u = flow velocity ($m\ s^{-1}$), D = tube diameter (m), ρ = density ($kg\ m^{-3}$), μ = viscosity (Pa s))

Moreover, decreasing the tube diameter increases the linear velocity of the fluid, hence lowering the tendency of particles to settle (see Equation 5).

$$V_l = \frac{Q}{\pi(D/2)^2} \quad (\text{Equation 5})$$

(V_l = linear velocity ($m\ s^{-1}$), D = tube diameter (m), Q = volumetric flow rate $m^3\ s^{-1}$)

D.4. Back-pressure regulation (BPR): the handling of solids has risen some concerns concerning the use of BPR, since they are not designed for such a purpose, especially over long periods. In the beginning, a Zaiput BPR-10 (composed of a membrane that restricts liquid flow until its pressure is matched), was used but it led to clogging after 2h30 processing time (Fig. S10d). A thick paste was obtained around the small apertures. That is why a simpler BPR configuration was selected, with the use of the Vapourtec BPR that only accounts for a rubber tube that is pressed (Fig. S10e). However, this choice was worse and clogging was obtained only after 30 min of processing time. Finally, a BPR with a larger internal volume, the Swagelok BPR (KCB Series, up to 25.8 bar, Fig. 10f), which is composed of a spring pushing a metallic part against the flow, has been used and at that moment, no clogging was observed during the long run experiment of 4 h. However, settling was observed within this BPR but this can be managed after carefully flushing this apparatus between each run. Therefore, the Zaiput BPR is suitable for shorter experiments while the Swagelok one is better for long run experiments.

D.5. Vibrators: since the strength of the turbulence decreases with distance from the oscillatory pump, it is important to add external pulsations to avoid solid settling,

especially before reaching the reactor. Three vibrators (Fig. S10c) were therefore put at strategic locations, namely before each pump and the BPR, to enable a homogeneous suspension before entering into these apparatuses, each possessing a large internal volume.

It is important to note that processing on a larger scale is expected to be easier, due to higher linear flow velocities.

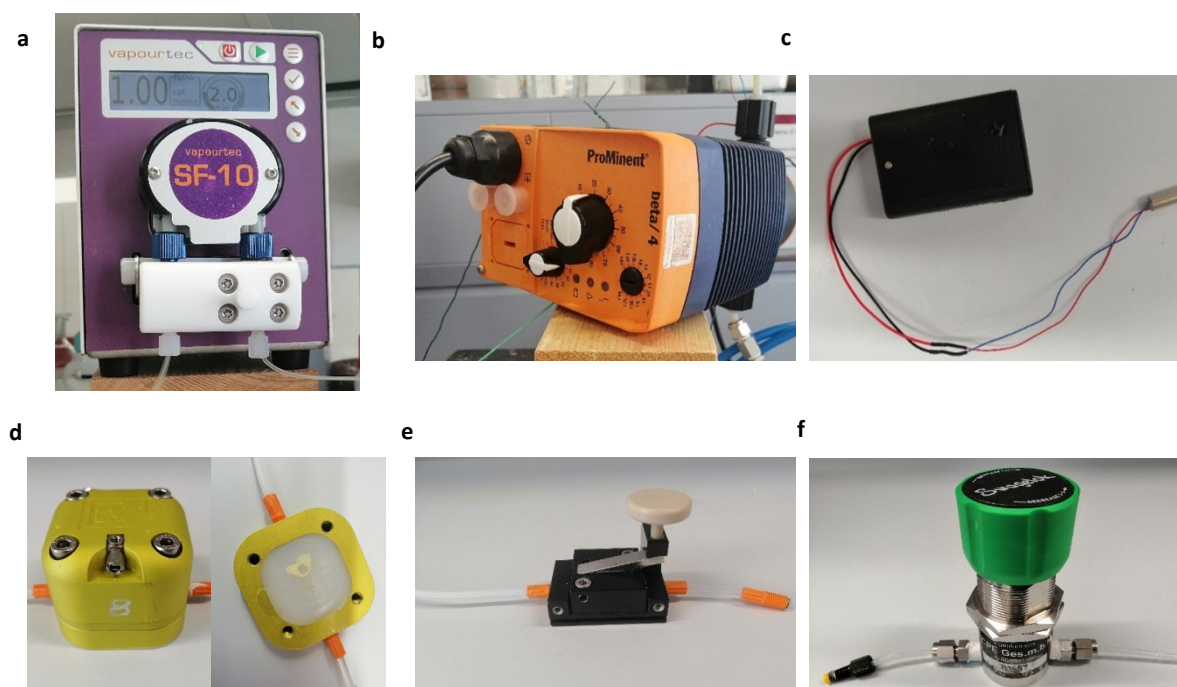


Fig. S10 Parts of the oscillatory flow set up. **(a)** metering peristaltic pump (SF-10, Vapourtec). **(b)** pulsator pump (Creaflow customized ProMinent (beta/4) pump with PTFE/carbon pump head). **(c)** Battery powered vibrator motor. **(d)** Left = Zaiput BPR (BPR-10); Right = Thick paste of Bi_2O_3 obtained during the clogging of the Zaiput BPR **(e)** Vapourtec BPR **(f)** Swagelok BPR

B.2.2. Residence time distribution

Minimizing the residence time distribution (RTD) is essential to ensure accurate control of the reaction, particularly since the solid and liquid phases are generally subject to a slightly different RTD. Since this characteristic is strongly affected by the oscillation parameters, experiments were conducted to see the effect of the pulsation amplitude and frequency. The aim of these experiments is to achieve a similar distribution between both reaction phases (measured by comparing relative concentration profile against conversion profile).

Decreasing frequency from 80% to 50% (Fig. S11a and Fig. S11b) provides a narrower distribution. A similar trend was observed at a lower amplitude pulsation (20% instead of 50%) when the frequency was decreased from 100% to 50 (Fig. S11c and S11d). A significant effect was seen when the amplitude was decreased from 50% to 20% (Fig. S11b and S11d). At a low amplitude, a similar trend was

observed between the internal standard area and the conversion, implying a narrower RTD. Therefore, a low oscillation amplitude was selected for the rest of the experiments, enabling both solid suspension and minimized RTD (20% amplitude and 50% frequency).

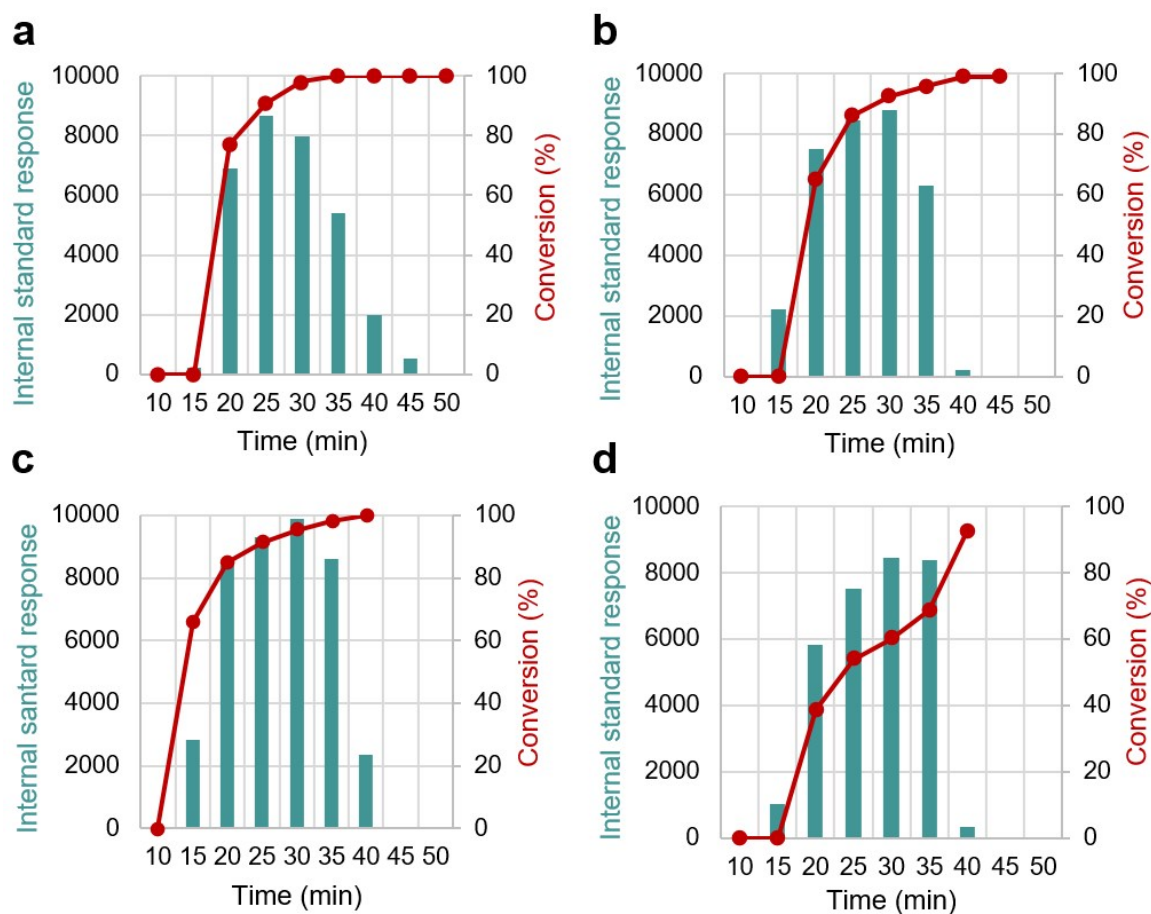


Fig. S11 Residence time distribution experiments performed with different oscillations. Conditions: **[1a]** = 0.675 M, **[2a]** = 0.5 M and **[2,6-lutidine]** = 0.5 M, solvent = acetone:PEG 400 (8:2), reaction volume = 25 mL, Bi_2O_3 loading = 2 mol%, 405 nm LED irradiation, pressure = 5 bar, temperature = 75 °C, residence time = 15 min, flow rate = 1 mL min^{-1} . **(a)** Frequency = 2.4 Hz (80%); amplitude = 0.265 mL (50%). **(b)** Frequency = 1.5 Hz (50%); amplitude = 0.265 mL (50%). **(c)** Frequency = 3 Hz (100%); amplitude = 0.12 mL (20%). **(d)** Frequency = 1.5 Hz (50%); amplitude = 0.12 mL (20%).

C. Process Mass Intensity (PMI) calculation

For the scale-out experiment detailed in the manuscript (250 mL solution), the PMI was calculated as follows:

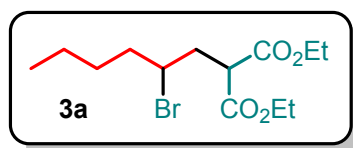
Table S3 List of individual masses used in the scale-out experiment, for calculation of the PMI.

Component	Mass used (g)
Acetone	156.8
PEG 400	56.5
2,6-lutidine	13.4
Diethyl bromomalonate	29.9
1-hexene	14.2
Product 3a	35.9
Total	306.7

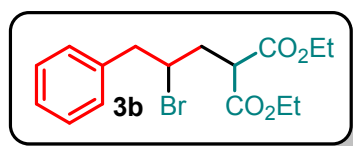
Note: due to catalyst recyclability (as demonstrated), the mass of Bi₂O₃ (1.2 g) was not considered for this calculation.

$$\text{PMI} = \text{total mass} / \text{product mass} = 306.7 / 35.9 = \mathbf{8.54}$$

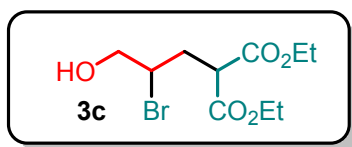
D. Scope – Procedures and characterization data



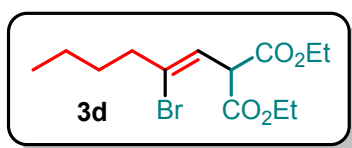
diethyl 2-(2-bromohexyl)malonate (3a): prepared according to the optimized flow procedure with 1-hexene **1a** (33.7 mmol, 1.35 equiv.) and diethyl bromomalonate **2a** (25 mmol, 1 equiv.) in a reaction mixture of 50 mL, with a residence time of 20 min and at 75 °C. Centrifugation (15 min at 5000 rpm), extraction (3 × 50 mL of diethyl ether), drying over Na₂SO₄, and automated flash chromatography on silica gel (40-60 petroleum ether:ethyl acetate, 95:5) were performed as purification steps. The corresponding product **3a** was obtained as a pale yellow oil (7.6 g, 94% yield). ¹H NMR (300 MHz, CDCl₃) δ 4.34 – 4.10 (m, 4H), 3.99 (dtd, *J* = 10.2, 6.5, 3.1 Hz, 1H), 3.78 (dd, *J* = 10.2, 4.2 Hz, 1H), 2.46 (ddd, *J* = 14.9, 10.2, 3.1 Hz, 1H), 2.24 (ddd, *J* = 14.8, 10.6, 4.3 Hz, 1H), 1.99 – 1.75 (m, 2H), 1.48 (dddd, *J* = 29.8, 14.8, 8.5, 6.2 Hz, 2H), 1.41 – 1.17 (m, 8H), 0.90 (t, *J* = 7.2 Hz, 3H). ¹³C NMR (75 MHz, CDCl₃) δ 169.2, 169.0, 61.8, 61.8, 55.2, 50.8, 39.3, 38.0, 29.7, 22.2, 14.2, 14.2, 14.0. HRMS (ESI, positive mode) calculated for C₁₃H₂₃Br^[79]O₄ (M+H)⁺: 323.0852, found: 323.0849



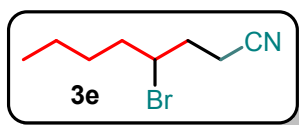
diethyl 2-(2-bromo-3-phenylpropyl)malonate (3b): prepared according to the optimized flow procedure with allyl benzene **1b** (16.9 mmol, 1.35 equiv.) and diethyl bromomalonate **2a** (12.5 mmol, 1 equiv.) in a reaction mixture of 25 mL, with a residence time of 30 min and at 80 °C. Centrifugation (15 min at 5000 rpm), extraction (3 × 50 mL of diethyl ether), drying over Na₂SO₄ and automated flash chromatography on silica gel (40-60 petroleum ether:ethyl acetate, 95:5) were performed as purification steps. The corresponding product **3b** was obtained as a pale yellow oil (4.0 g, 90% yield). ¹H NMR (300 MHz, CDCl₃) δ 7.40 – 7.13 (m, 5H), 4.22 (tdd, *J* = 10.4, 8.3, 5.2 Hz, 5H), 3.82 (dd, *J* = 10.4, 4.0 Hz, 1H), 3.23 (d, *J* = 7.0 Hz, 2H), 2.72 – 2.45 (m, 1H), 2.26 (ddd, *J* = 14.9, 10.9, 4.0 Hz, 1H), 1.27 (m, *J* = 7.3 Hz, 6H); ¹³C NMR (75 MHz, CDCl₃) δ 168.9, 168.6, 137.7, 129.2, 128.5, 127.0, 61.7, 61.6, 54.1, 50.6, 45.8, 37.2, 14.0; HRMS (ESI, positive mode) calculated for C₁₆H₂₁Br^[79]O₄ (M+H)⁺: 357.0696, found: 357.0688



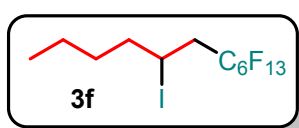
diethyl 2-(2-bromo-3-hydroxypropyl)malonate (3c): prepared according to the optimized flow procedure with allyl alcohol **1c** (16.9 mmol, 1.35 equiv.) and diethyl bromomalonate **2a** (12.5 mmol, 1 equiv.) in a reaction mixture of 25 mL, with a residence time of 30 min and at 80 °C. Centrifugation (15 min at 5000 rpm), extraction (3 × 50 mL of diethyl ether), drying over Na₂SO₄, and automated flash chromatography on silica gel (40-60 petroleum ether:ethyl acetate, 50:50) were performed as purification steps. The corresponding product **3c** was obtained as a pale yellow oil (2.45 g, 66% yield). ¹H NMR (300 MHz, CDCl₃) δ 4.38 – 4.06 (m, 5H), 3.84 – 3.75 (m, 2H), 3.72 (dd, *J* = 9.5, 5.0 Hz, 1H), 2.58 – 2.23 (m, 2H), 1.26 (m, *J* = 7.1, 3.6, 2.2 Hz, 6H); ¹³C NMR (75 MHz, CDCl₃) δ 169.0, 168.7, 66.9, 61.9, 61.8, 55.4, 50.0, 33.6, 14.0; HRMS (ESI, positive mode) calculated for C₁₀H₁₇Br^[79]O₅ (M+H)⁺: 297.0332, found: 297.0326



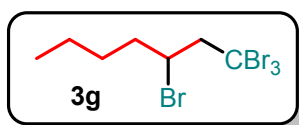
diethyl (Z)-2-(2-bromohex-1-en-1-yl)malonate (3d): prepared according to the optimized flow procedure with 1-hexyne **1d** (16.9 mmol, 1.35 equiv.) and diethyl bromomalonate **2a** (12.5 mmol, 1 equiv.) in a reaction mixture of 25 mL, with a residence time of 30 min and at 80 °C. Centrifugation (15 min at 5000 rpm), extraction (3 × 50 mL of diethyl ether), drying over Na₂SO₄, and automated flash chromatography on silica gel (40-60 petroleum ether:ethyl acetate, 95:5) were performed as purification steps. The corresponding product **3d** was obtained as a pale yellow oil (2.0 g, 55% yield). ¹H NMR (300 MHz, CDCl₃) δ 5.78 – 5.61 (m, 1H), 4.21 (qd, *J* = 7.1, 5.3 Hz, 4H), 2.49 (m, 2H), 2.09 (m, 2H), 1.72 – 1.49 (m, 2H), 1.39 – 1.21 (m, 8H), 0.92 (t, *J* = 7.4 Hz, 3H). ¹³C NMR (75 MHz, CDCl₃) δ 167.3, 133.8, 120.6, 61.9, 55.0, 41.3, 30.0, 21.3, 14.0, 13.7. HRMS (ESI, positive mode) calculated for C₁₃H₂₁Br^[79]O₄ (M+H)⁺: 321.0696, found: 321.0696



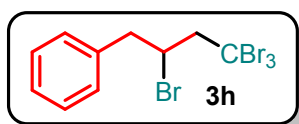
4-bromooctanenitrile (3e): prepared according to the optimized flow procedure with 1-hexene **1a** (16.9 mmol, 1.35 equiv.) and bromoacetonitrile **2b** (12.5 mmol, 1 equiv.) in a reaction mixture of 25 mL, with a residence time of 30 min and at 80 °C. Centrifugation (15 min at 5000 rpm), extraction (3 × 50 mL of diethyl ether), and drying over Na₂SO₄ were performed as purification steps. The corresponding product **3e** was obtained as a pale yellow oil (2.5 g, 95% yield). The characterization of the compound matches the data reported in the literature.⁵³



1,1,1,2,2,3,3,4,4,5,5,6,6-tridecafluoro-8-iodododecane (3f): prepared according to the optimized flow procedure with 1-hexene **1a** (16.9 mmol, 1.35 equiv.) and perfluorohexyl iodide **2c** (12.5 mmol, 1 equiv.) in a reaction mixture of 25 mL, with a residence time of 20 min and at 75 °C. Centrifugation (15 min at 5000 rpm), extraction (3 × 50 mL of diethyl ether), and drying over Na₂SO₄ were performed as purification steps. The corresponding product **3f** was obtained as a colorless oil (6.5 g, 97% yield). The characterization of the compound matches the data reported in the literature.⁵⁴



1,1,1,3-tetrabromoheptane (3g): prepared according to the optimized flow procedure with 1-hexene **1a** (16.9 mmol, 1.35 equiv.) and carbontetrabromide **2d** (12.5 mmol, 1 equiv.) in a reaction mixture of 25 mL, with a residence time of 20 min and at 75 °C. Centrifugation (15 min at 5000 rpm), extraction (3 × 50 mL of diethyl ether), drying over Na₂SO₄, and automated flash chromatography on silica gel (40-60 petroleum ether:ethyl acetate, 95:5) were performed as purification steps. The corresponding product **3g** was obtained as a pale orange oil (2.7 g, 52% yield). ¹H NMR (300 MHz, CDCl₃) δ 4.37 – 4.10 (m, 1H), 3.85 (dd, *J* = 16.2, 4.5 Hz, 1H), 3.56 (dd, *J* = 16.2, 4.8 Hz, 1H), 2.23 – 1.91 (m, 2H), 1.72 – 1.47 (m, 2H), 2.3 – 1.47 (m, 2H), 0.96 (t, *J* = 7.2 Hz, 3H). ¹³C NMR (75 MHz, CDCl₃) δ 66.9, 52.0, 39.5, 36.4, 29.5, 22.0, 13.8



(2,4,4,4-tetrabromobutyl)benzene (3h): prepared according to the optimized flow procedure with allyl benzene **1b** (16.9 mmol, 1.35 equiv.) and carbontetrabromide **2d** (12.5 mmol, 1 equiv.) in a reaction mixture of 25 mL, with a residence time of 20 min and at 75 °C. Centrifugation (15 min at 5000 rpm), extraction (3 × 50 mL of diethyl ether), drying over Na₂SO₄, and automated flash chromatography on silica gel (40-60 petroleum ether:ethyl acetate, 50:50) were performed as purification steps. The corresponding product **3h** was obtained as a colorless oil (3.2 g, 57% yield). The characterization of the compound matches the data reported in the literature.^{S5}

E. NMR spectra

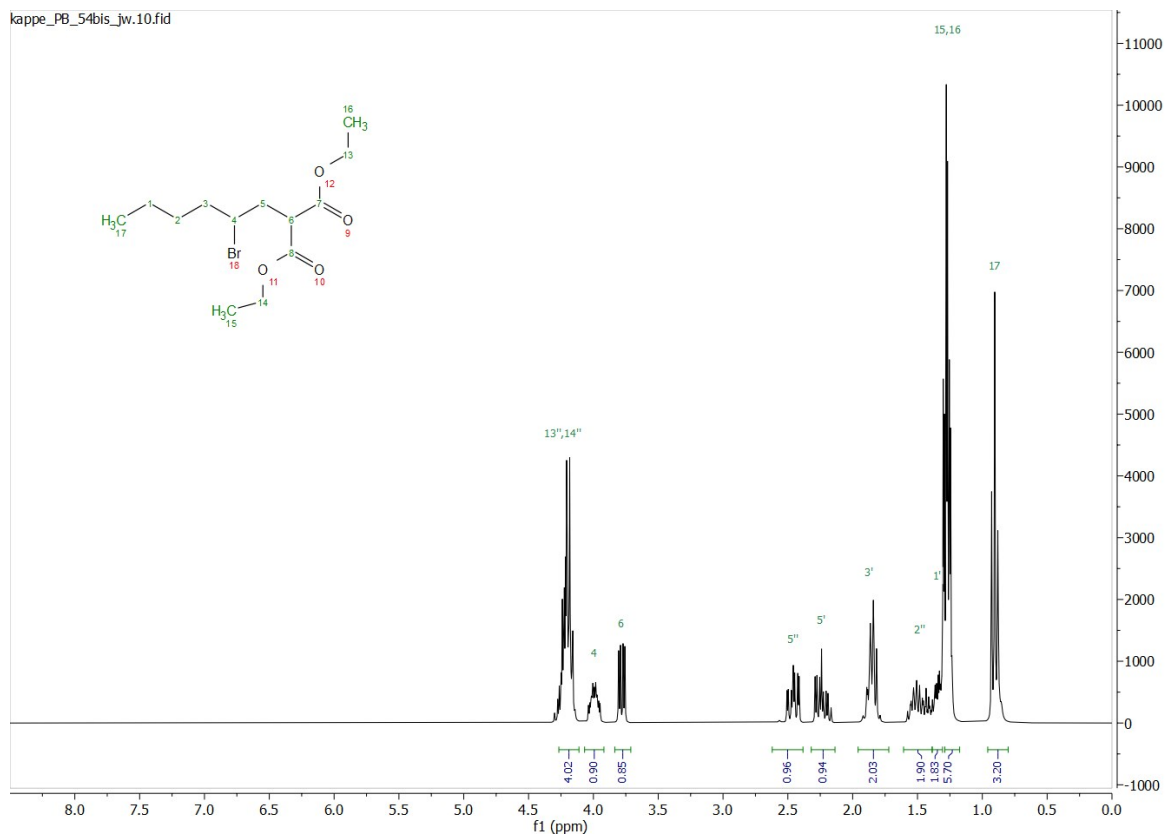


Fig. S12 ^1H NMR spectrum (300 MHz) of diethyl 2-(2-bromoethyl)malonate (3a) in CDCl_3 .

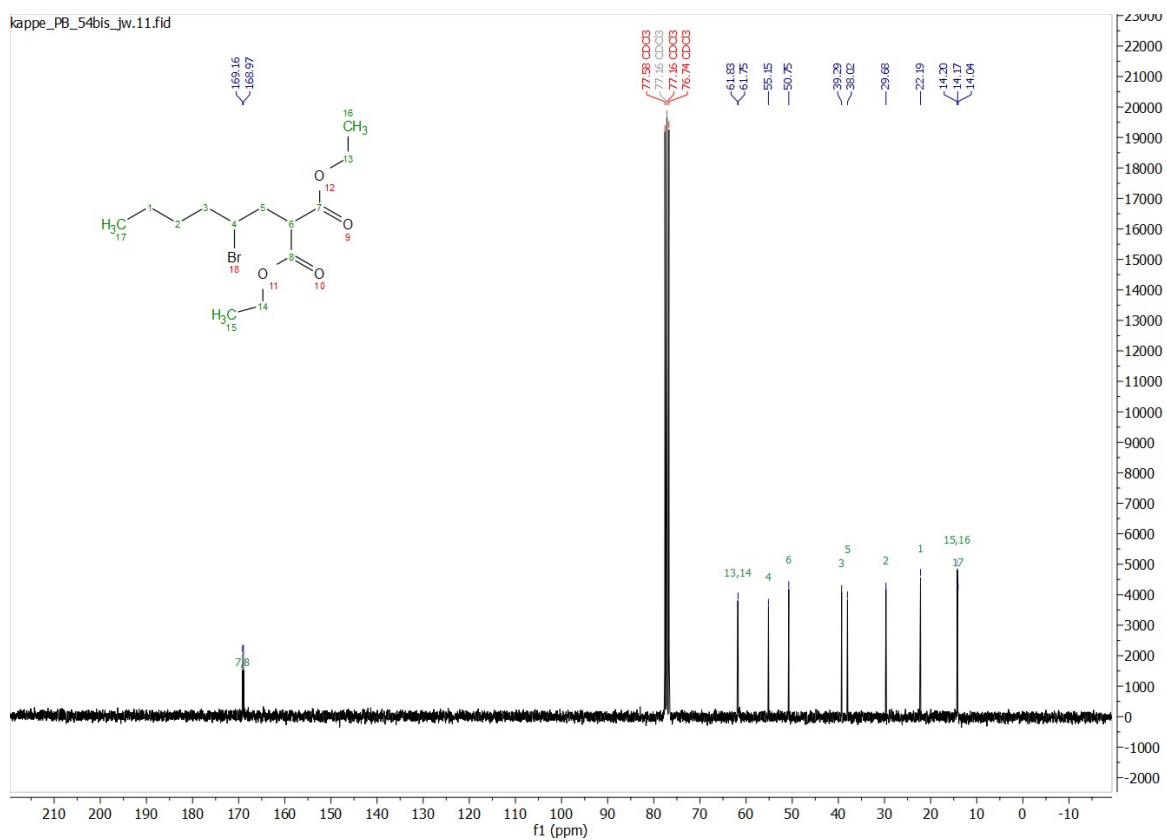


Fig. S13 ^{13}C NMR spectrum (75 MHz) of diethyl 2-(2-bromoethyl)malonate (3a) in CDCl_3 .

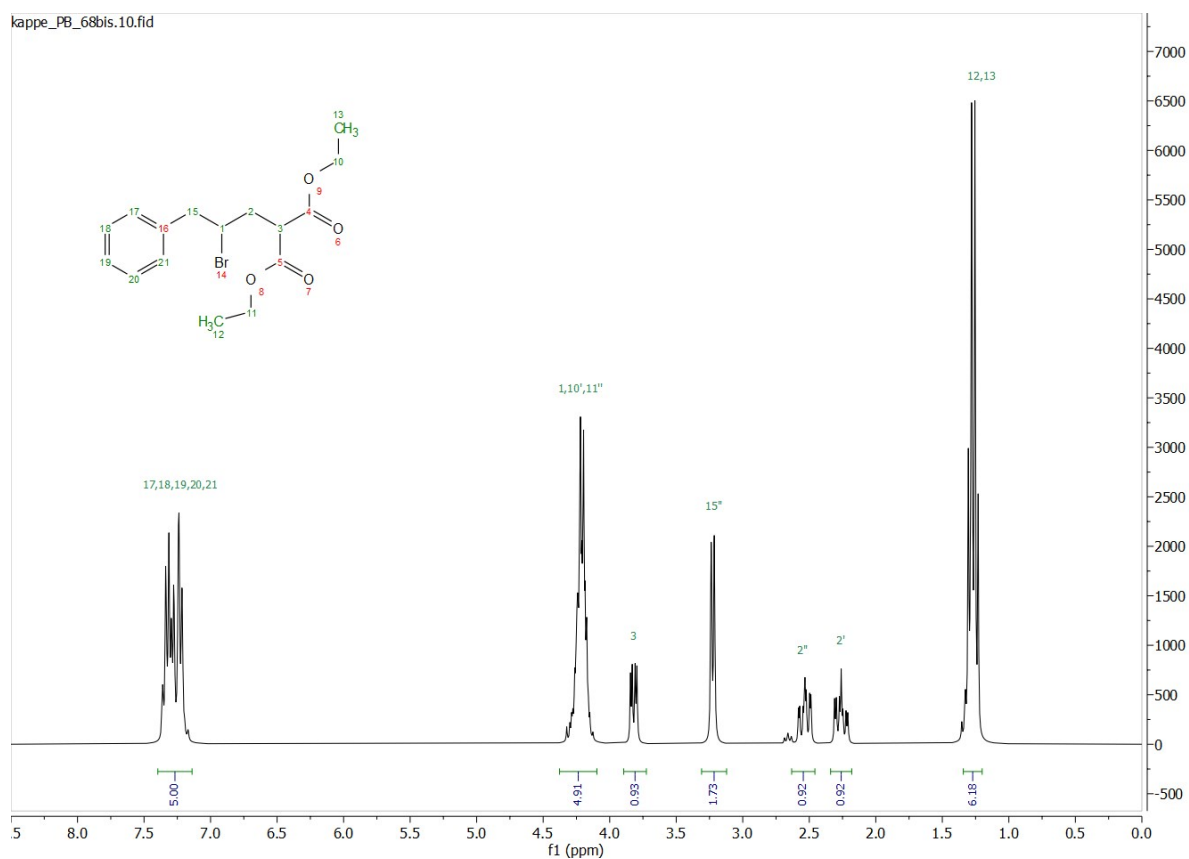


Fig. S14 ^1H NMR spectrum (300 MHz) of diethyl 2-(2-bromo-3-phenylpropyl) (**3b**) in CDCl_3

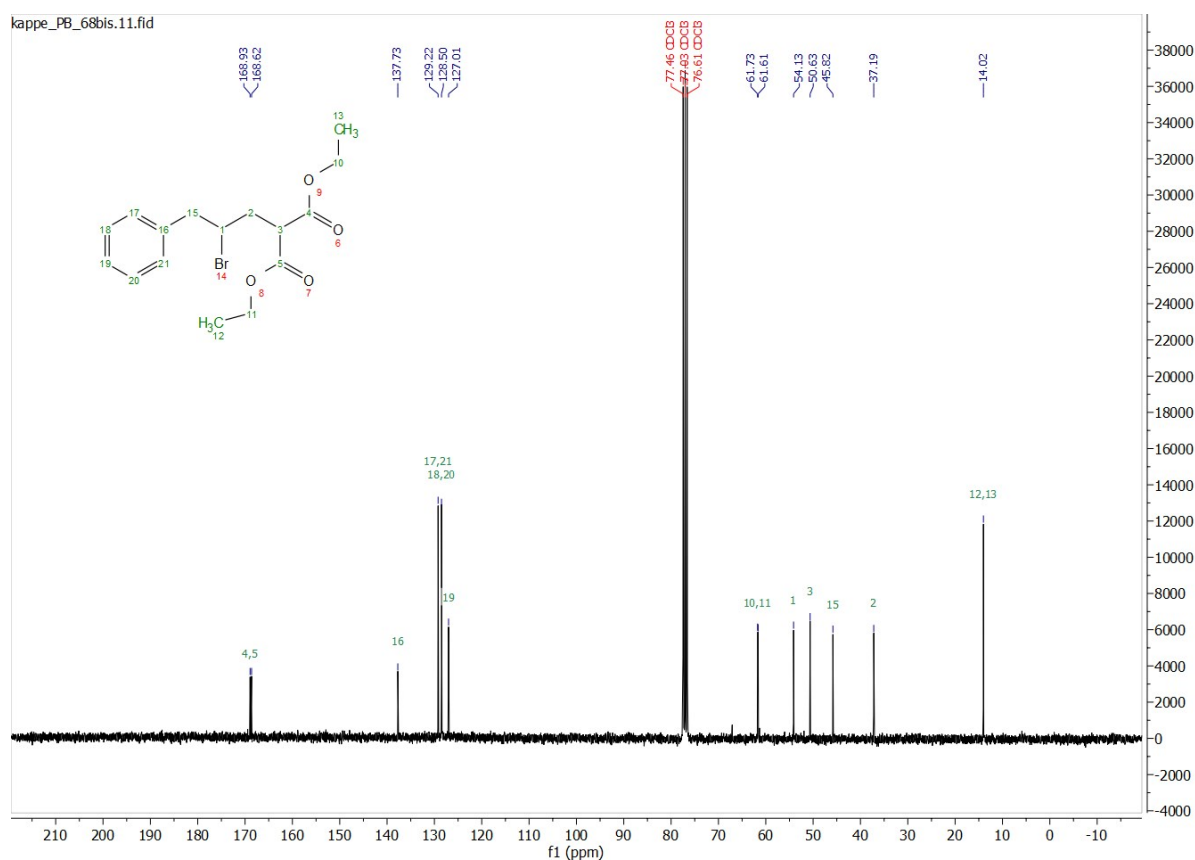
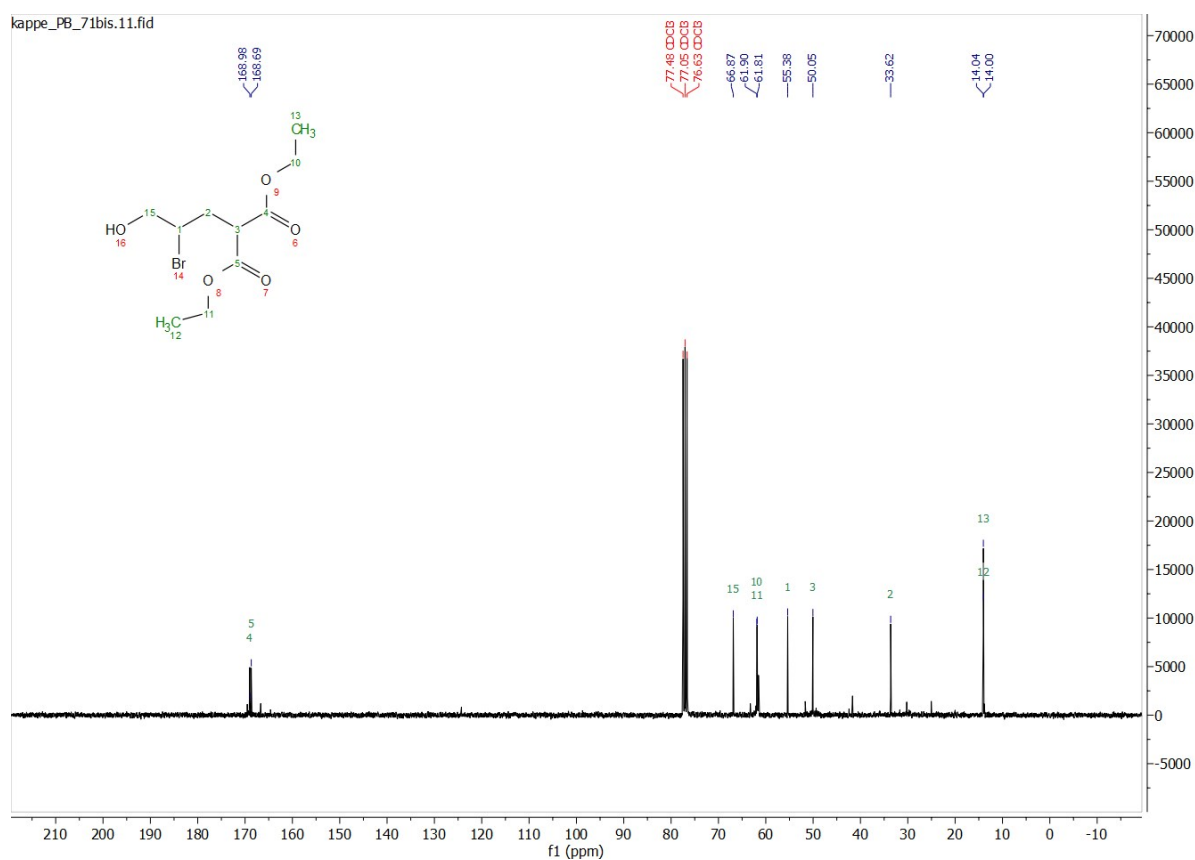
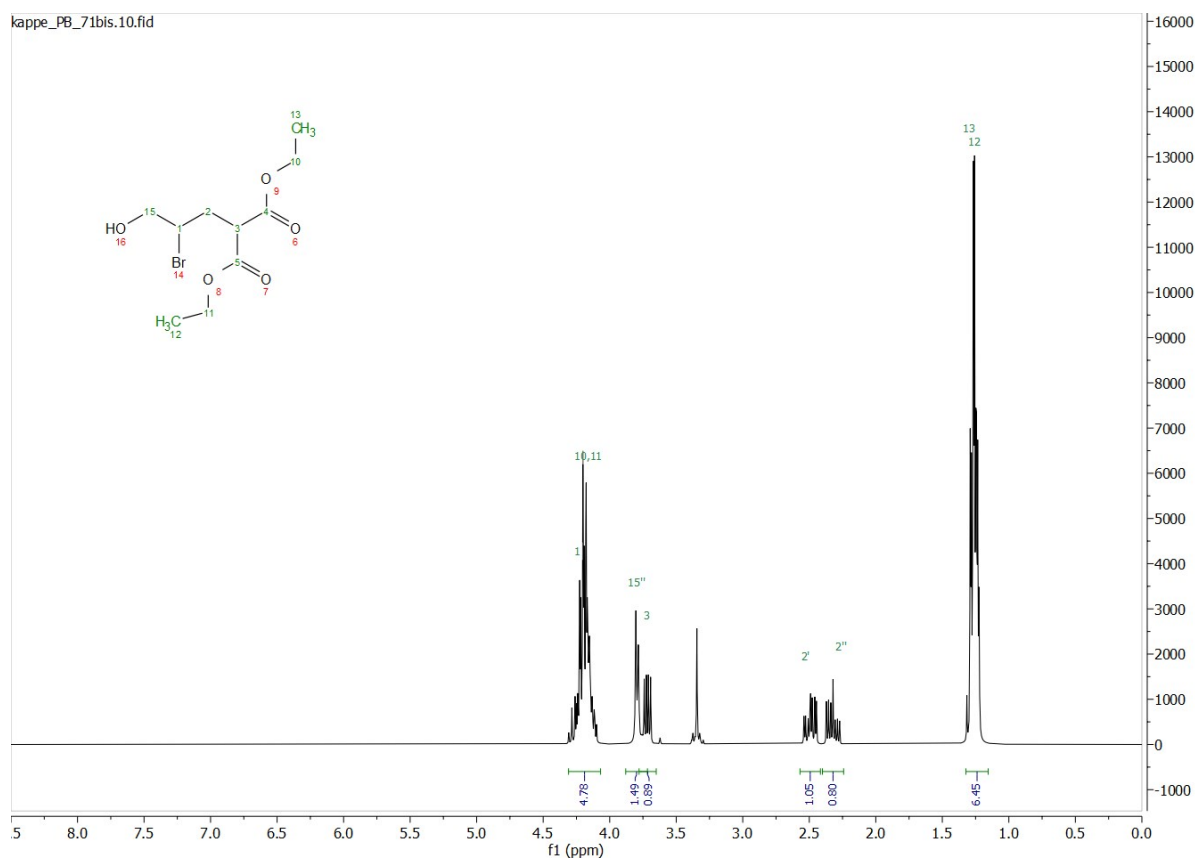
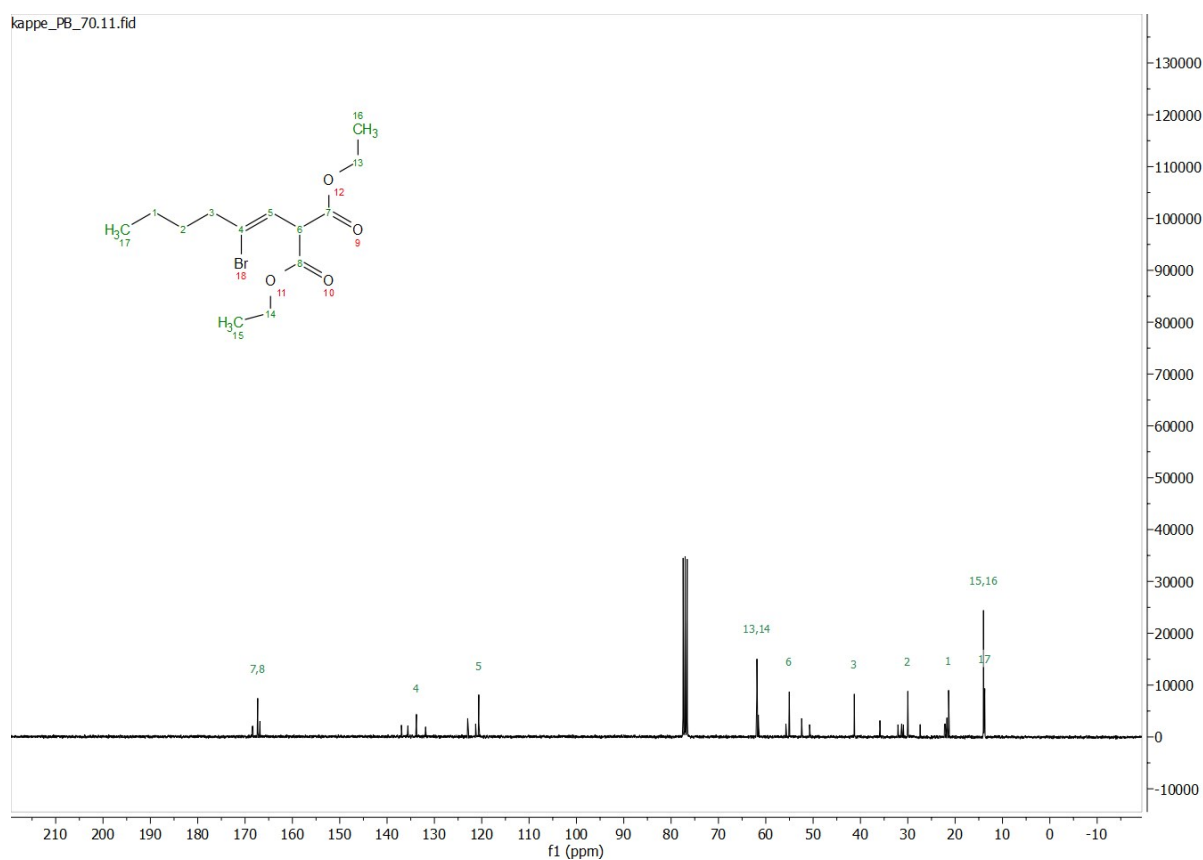
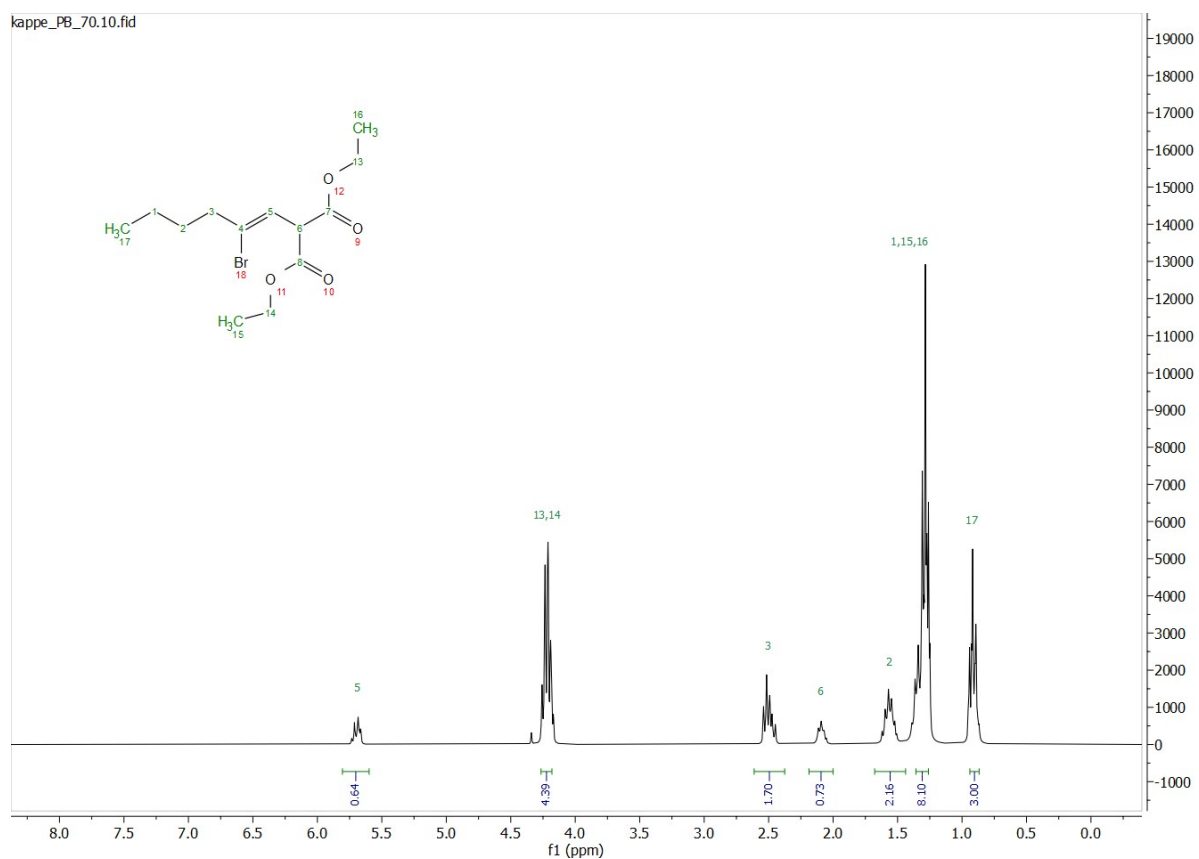
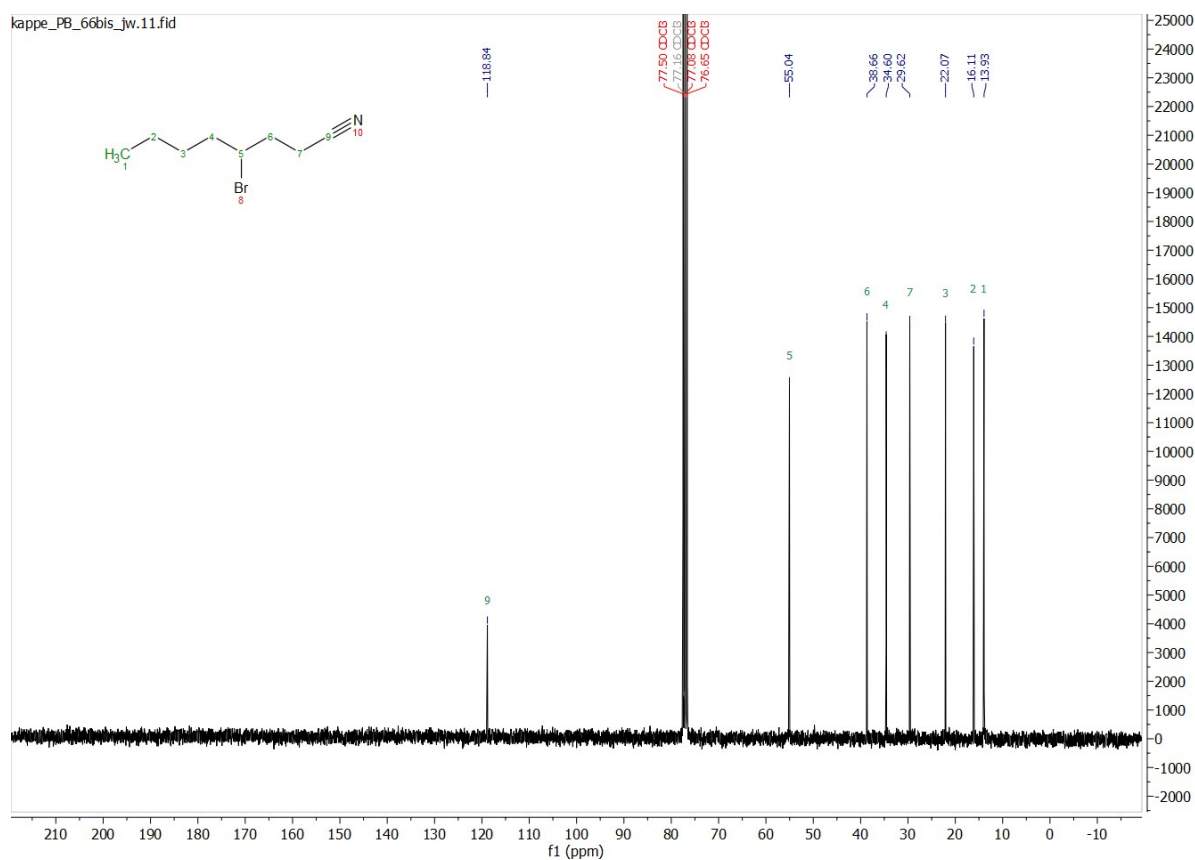
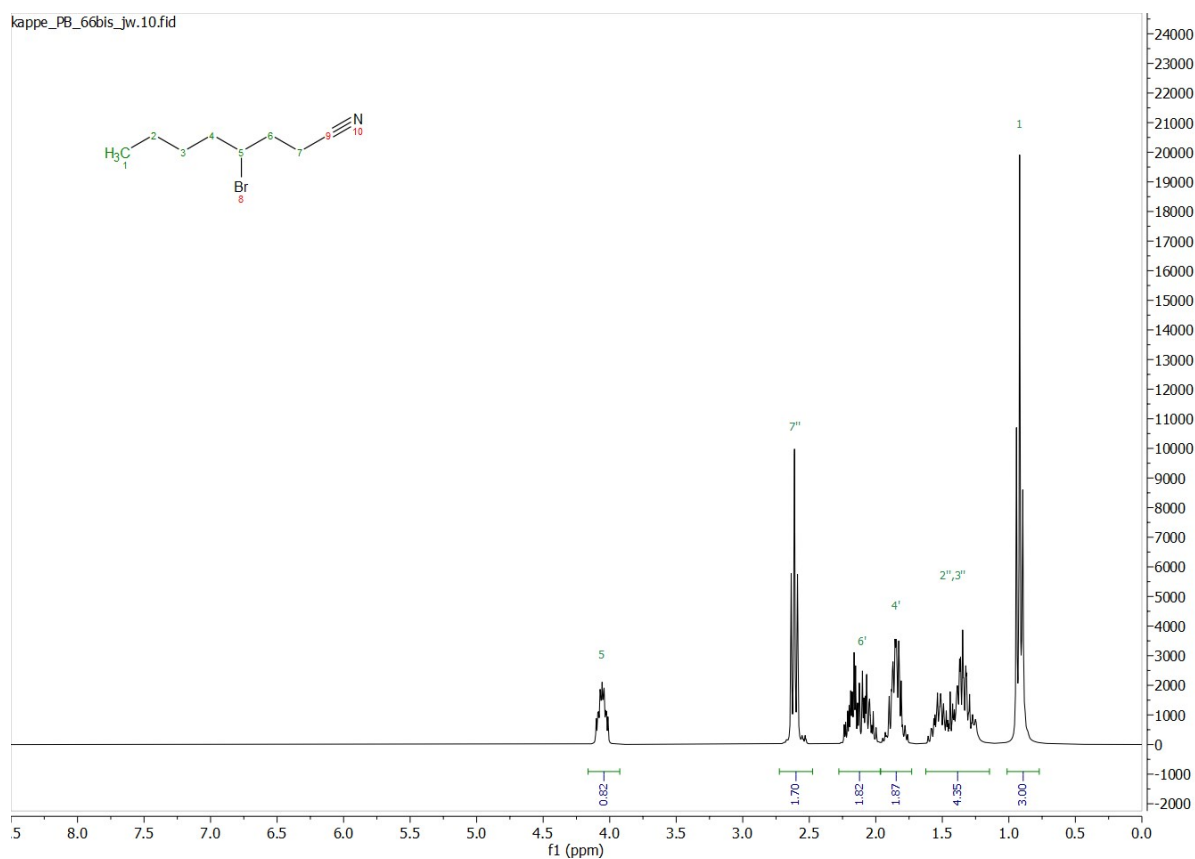
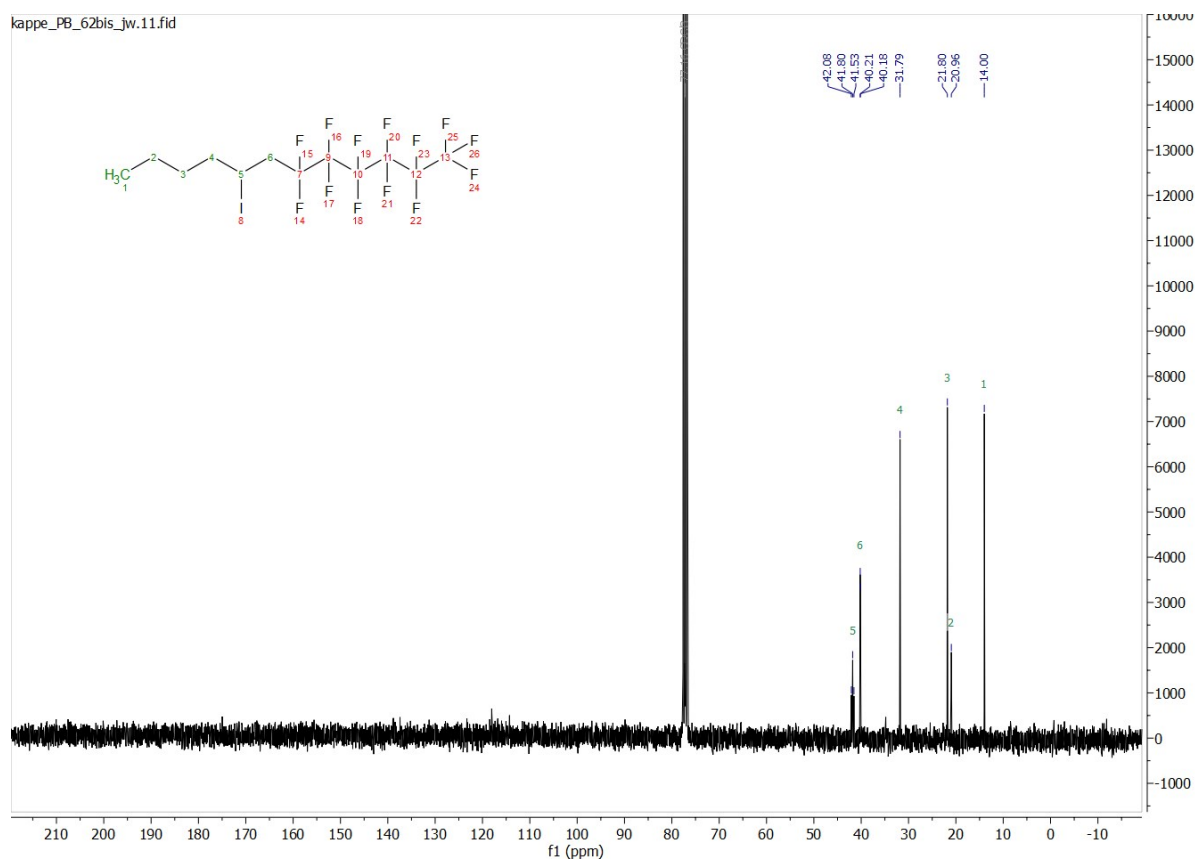
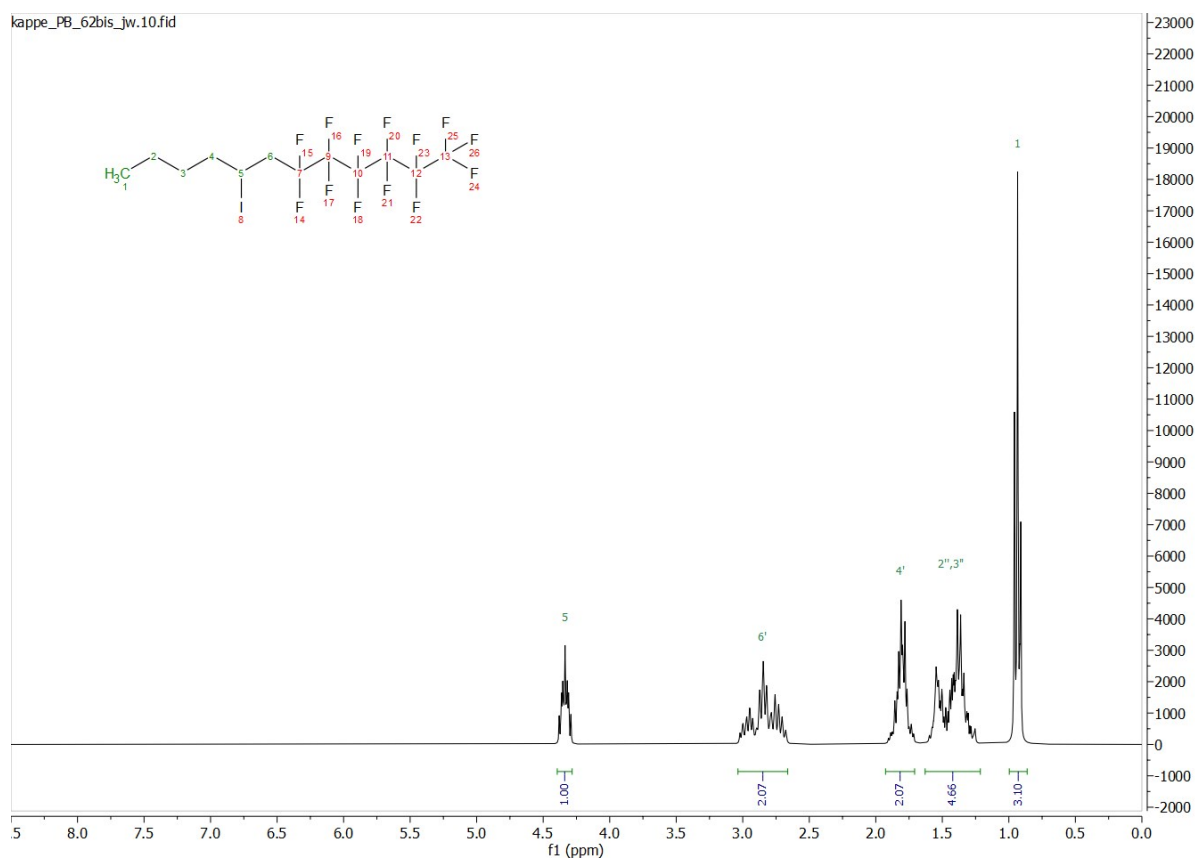


Fig. S15 ^{13}C NMR spectrum (75 MHz) of diethyl 2-(2-bromo-3-phenylpropyl) (**3b**) in CDCl_3









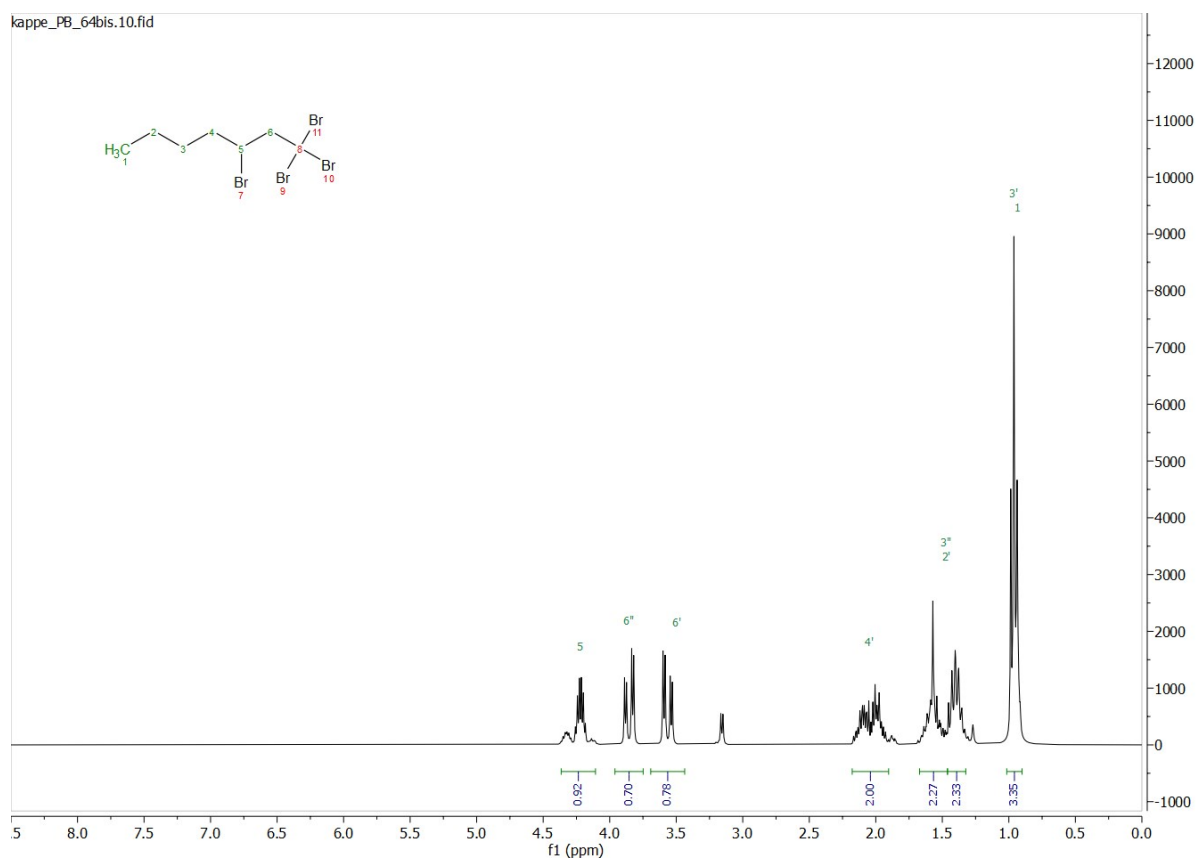


Fig. S24 ^1H NMR spectrum (300 MHz) of 1,1,1,3-tetrabromoheptane (**3g**) in CDCl_3

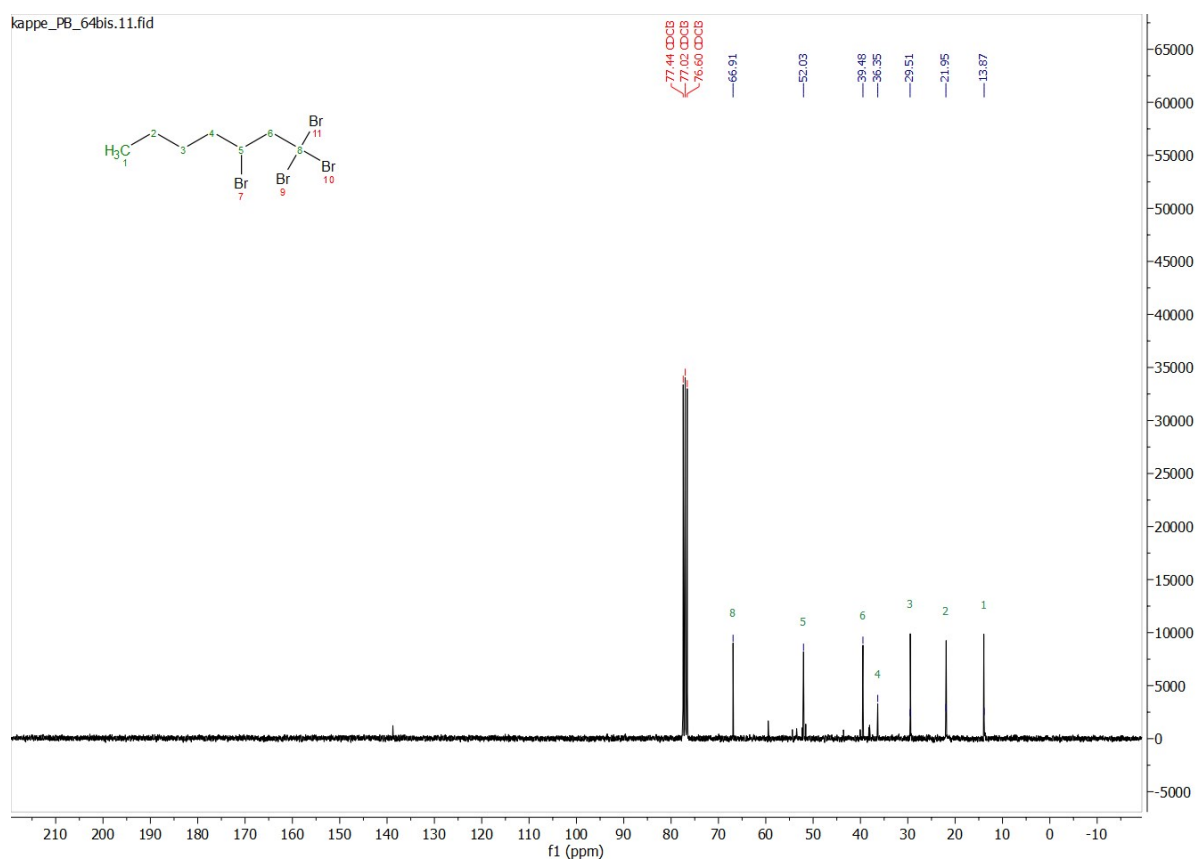


Fig. S25 ^{13}C NMR spectrum (75 MHz) of 1,1,1,3-tetrabromoheptane (**3g**) in CDCl_3

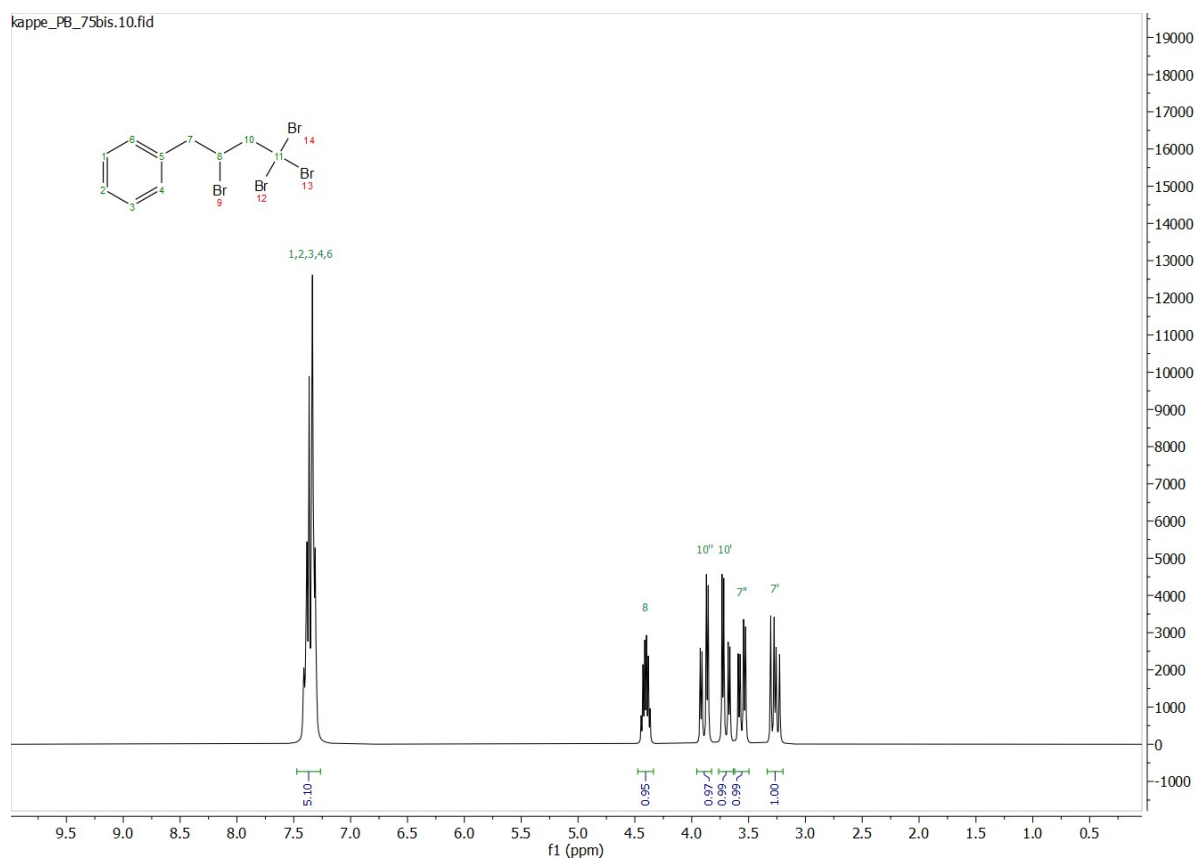


Fig. S26 ¹H NMR spectrum (300 MHz) of (2,4,4,4-tetrabromobutyl)benzene (3h) in CDCl₃

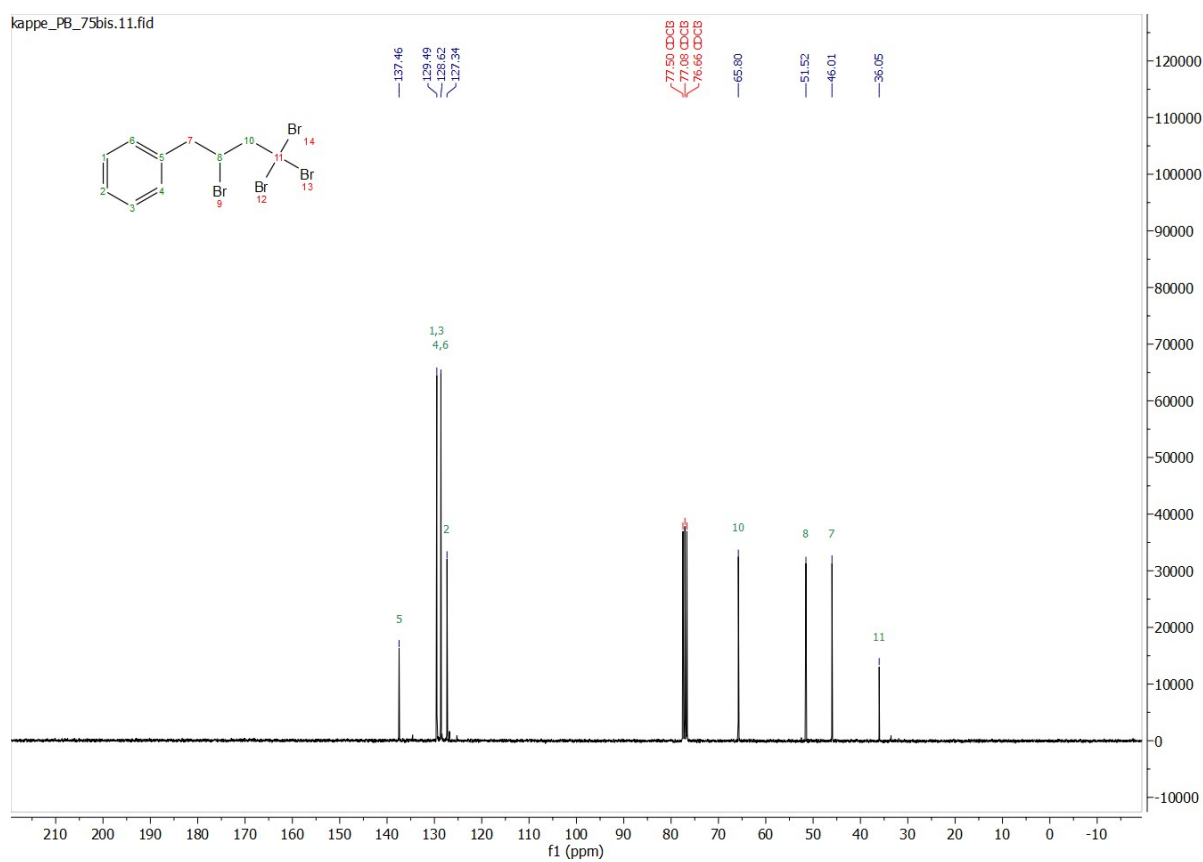


Fig. S27 ¹³C NMR spectrum (75 MHz) of (2,4,4,4-tetrabromobutyl)benzene (3h) in CDCl₃

F. References

- S1 M. Schoenitz, L. Grundemann, W. Augustin and S. Scholl, *Chem. Commun.*, 2015, **51**, 8213–8228.
- S2 D. Slavnić, B. Bugarski and N. Nikačević, *Chem. Eng. Process.*, 2019, **135**, 108–119.
- S3 E. Voutyritsa, I. Triandafillidi and C. G. Kokotos, *ChemCatChem*, 2018, **10**, 2466–2470.
- S4 C. Rosso, G. Filippini and M. Prato, *Chem. - Eur. J.*, 2019, **25**, 16032–16036.
- S5 P. Riente and M. A. Pericàs, *ChemSusChem*, 2015, **5**, 1841–1844.